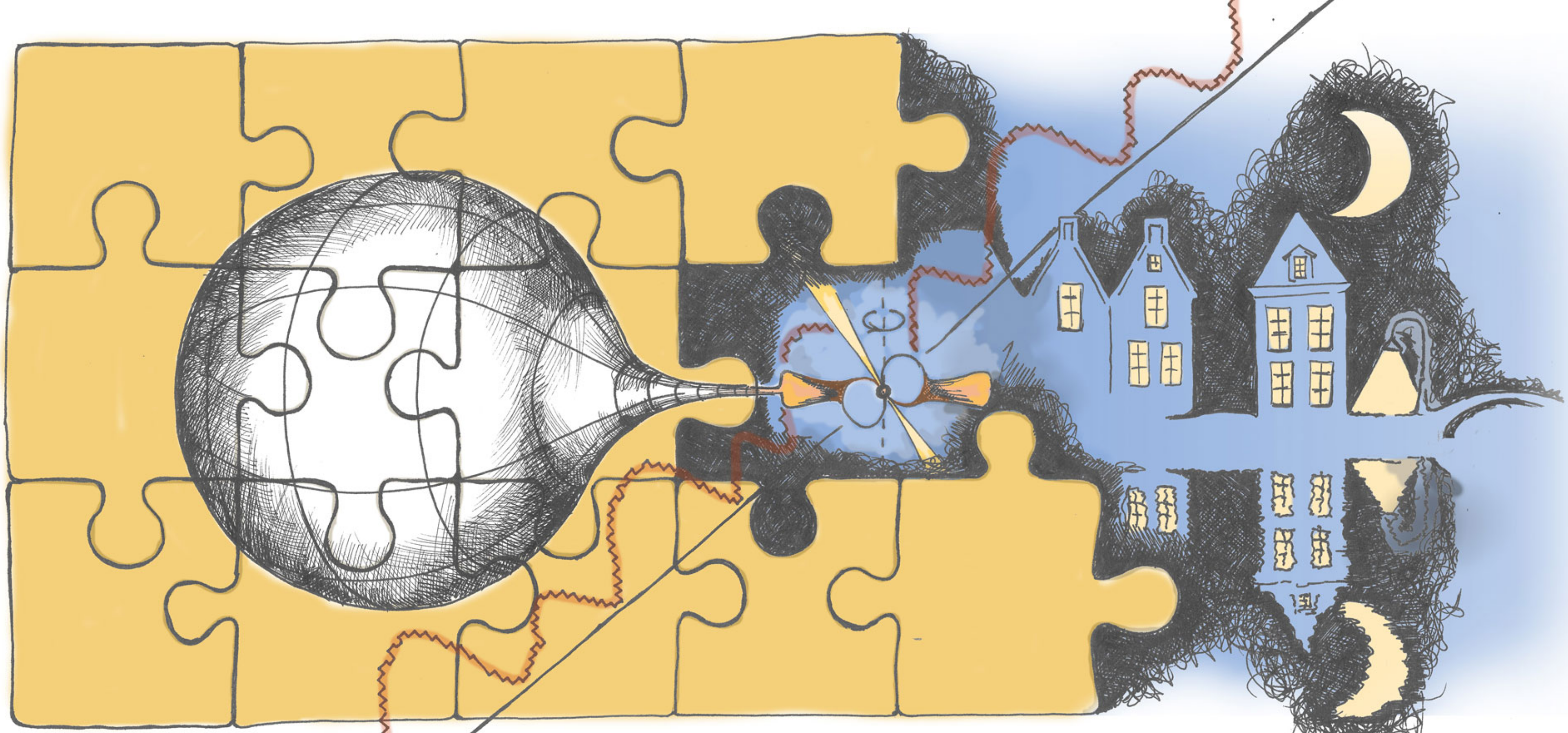

Extreme Accretion onto Strongly Magnetized Neutron Stars

Alexander Mushtukov

12 April 2021

Universiteit Leiden

Ultraluminous X-ray Sources (ULXs)

- Off-center bright X-ray sources in nearby galaxies
- Discovered with Einstein X-ray observatory 30 years ago
- X-ray luminosity: $L_x = 10^{39}$-10^{41} erg s^{-1}

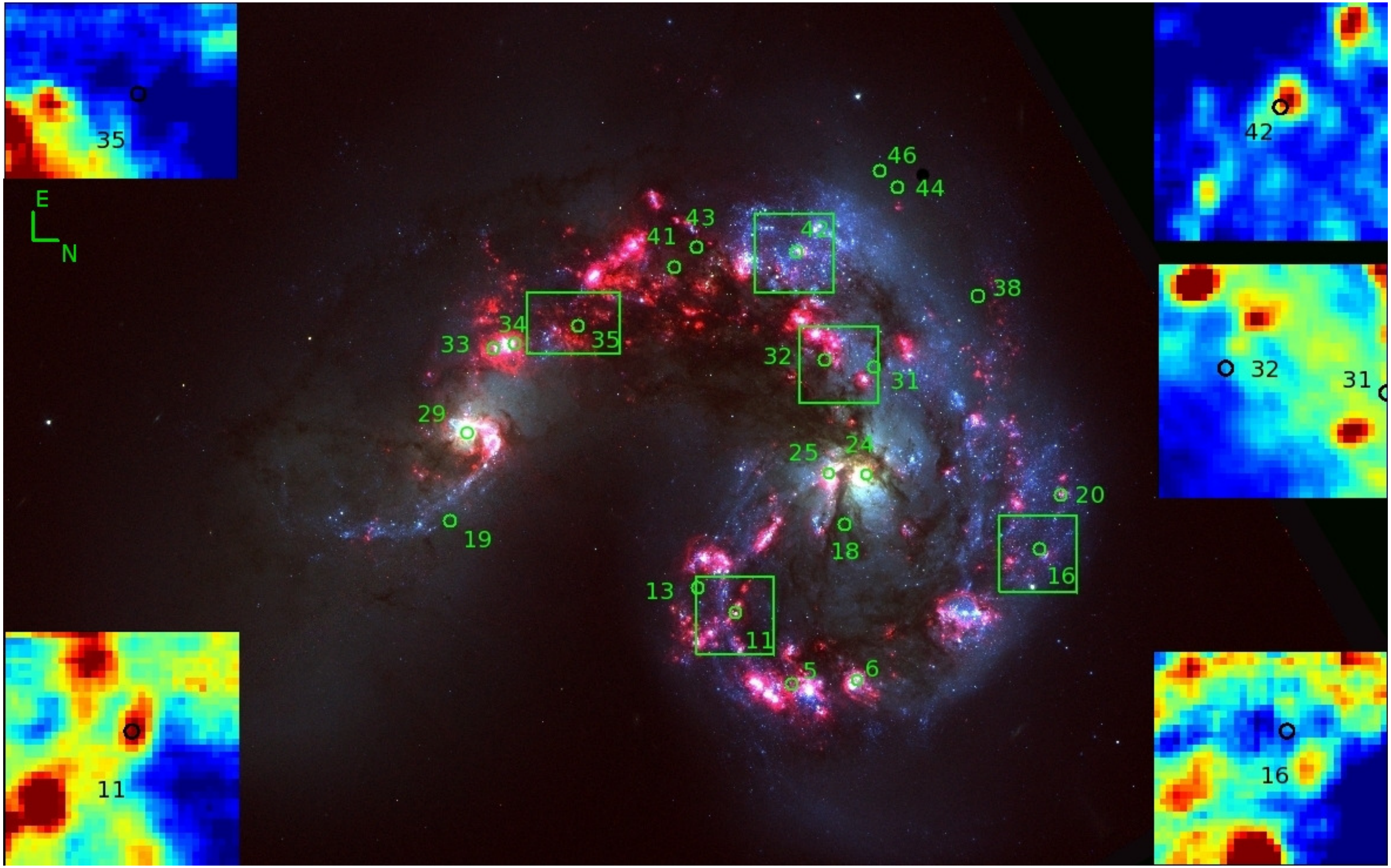

Poutanen+, 2013, MNRAS, 432

Pulsations from ULX in M82

and the modulation arises from its binary orbit. The pulsed flux alone corresponds to an X-ray luminosity in the 3–30 kiloelectronvolt range of 4.9×10^{39} ergs per second. The pulsating source is spatially coincident with a variable source[4] that can reach an X-ray luminosity in the 0.3–10 kiloelectronvolt range of 1.8×10^{40} ergs per second[1]. This

Pulse period ~1.37 sec

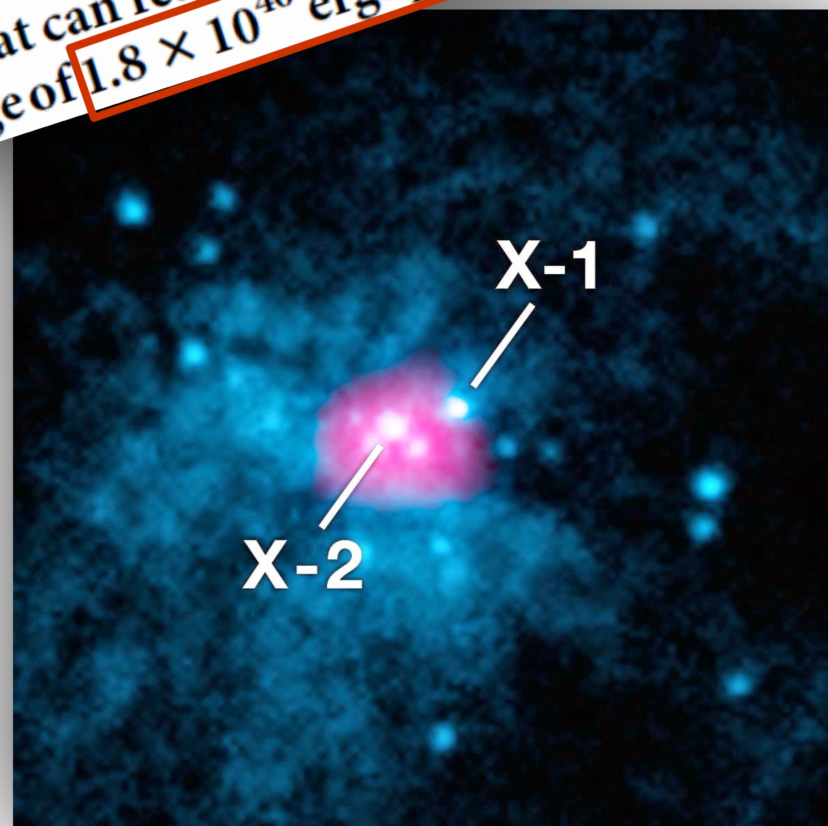

Bachetti+ 2014, Nature

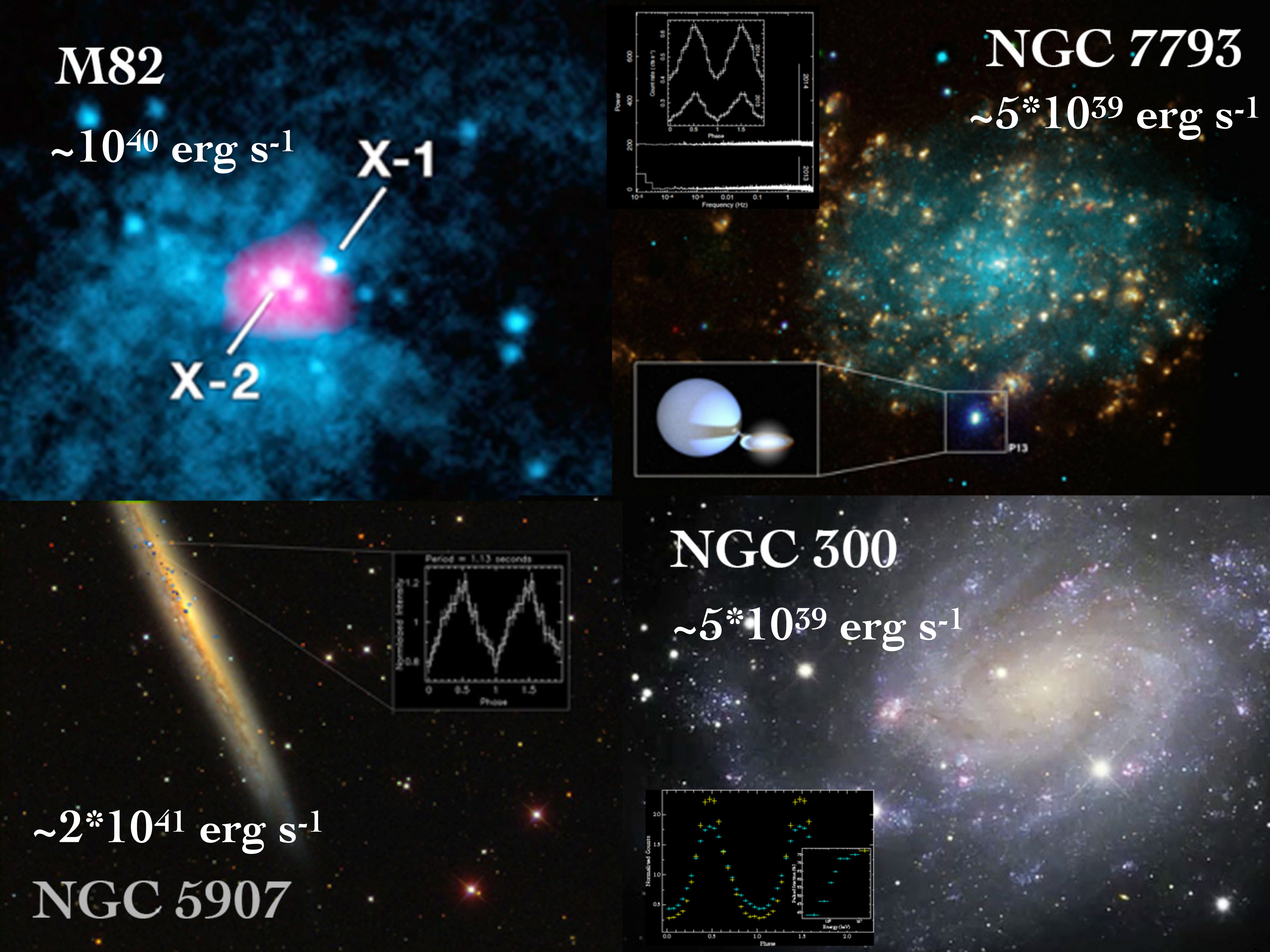

M82
~10^{40} erg s^{-1}
X-1
X-2
NGC 7793
~$5*10^{39}$ erg s^{-1}
P13
Frequency (Hz)
Power
Phase
NGC 300
~$5*10^{39}$ erg s^{-1}
Period = 1.13 seconds
Normalized Intensity
Phase
~$2*10^{41}$ erg s^{-1}
NGC 5907

ULX-pulsars in a nutshell

name	M82 ULX2	NGC 7793 P13	NGC5907 ULX1	NGC300 ULX1
L_X (max) [erg s^{-1}]	1.8×10^{40}	5×10^{39}	10^{41}	4.7×10^{39}
P_s [s]	1.37	0.42	1.13	31.5
$\dot{\nu}$ [s^{-2}]	10^{-10}	4×10^{-11}	$4.\times10^{-9}$	5.6×10^{-10}
P_{orb} [d]	2.52	64	5.3	
M_2 [$M_\odot$]	≥ 5.2	$18-23$		

- Large pulsed fraction, 20-30%, in all objects
- Smooth pulse profiles
- Huge variations in luminosity
- Multi-colour blackbody spectrum
- No (or very week?) cyclotron lines

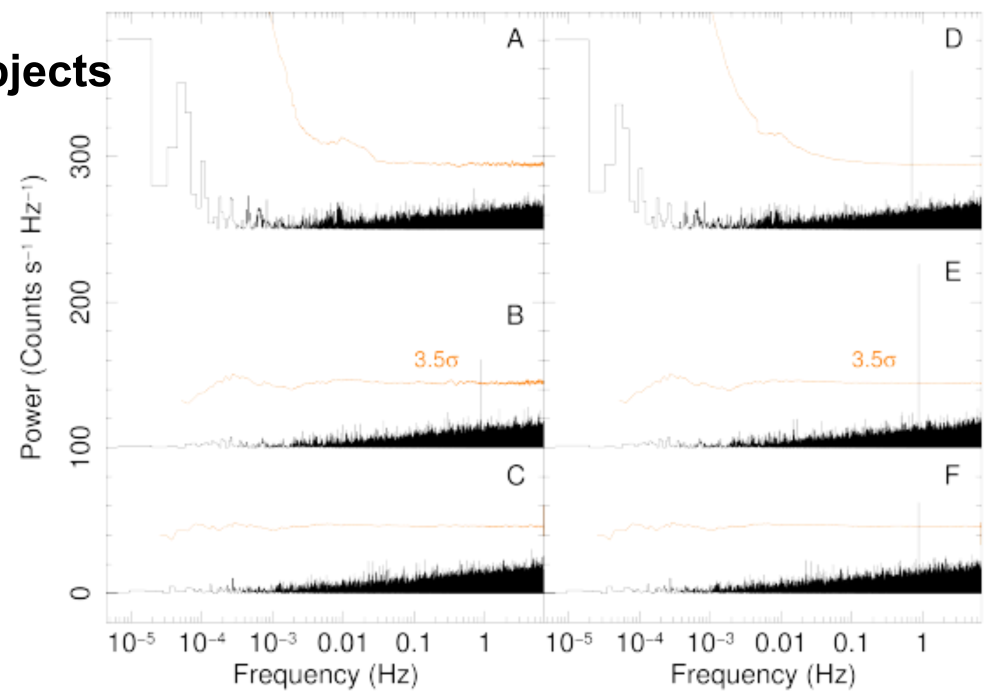

Bachetti+ 2014, Nature, 514
Israel+, 2017, Science, 355
Israel+, 2017, MNRAS, 466
Fürst+, 2016, ApJ, 831
Carpano+, 2018, MNRAS, 476

Neutron Stars

Product of supernova explosions

Mass density

$>10^{14}$ g cm^{-3}

The Highest Density in the Universe

Mass: 1.5 M_{sun}
Radius: 10 km

Magnetic fields

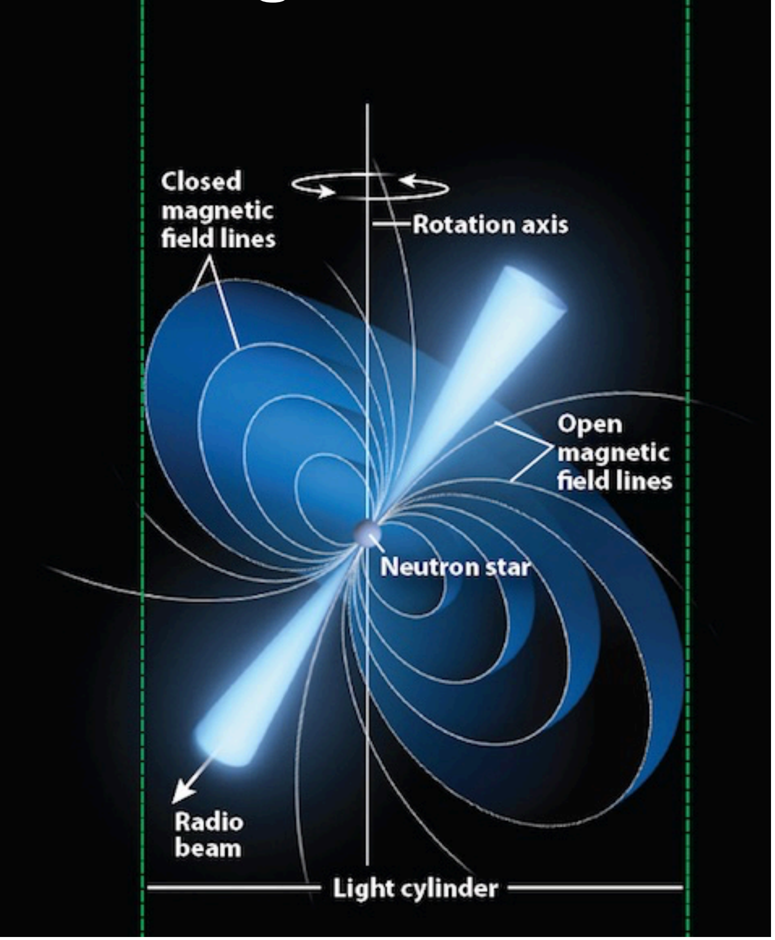

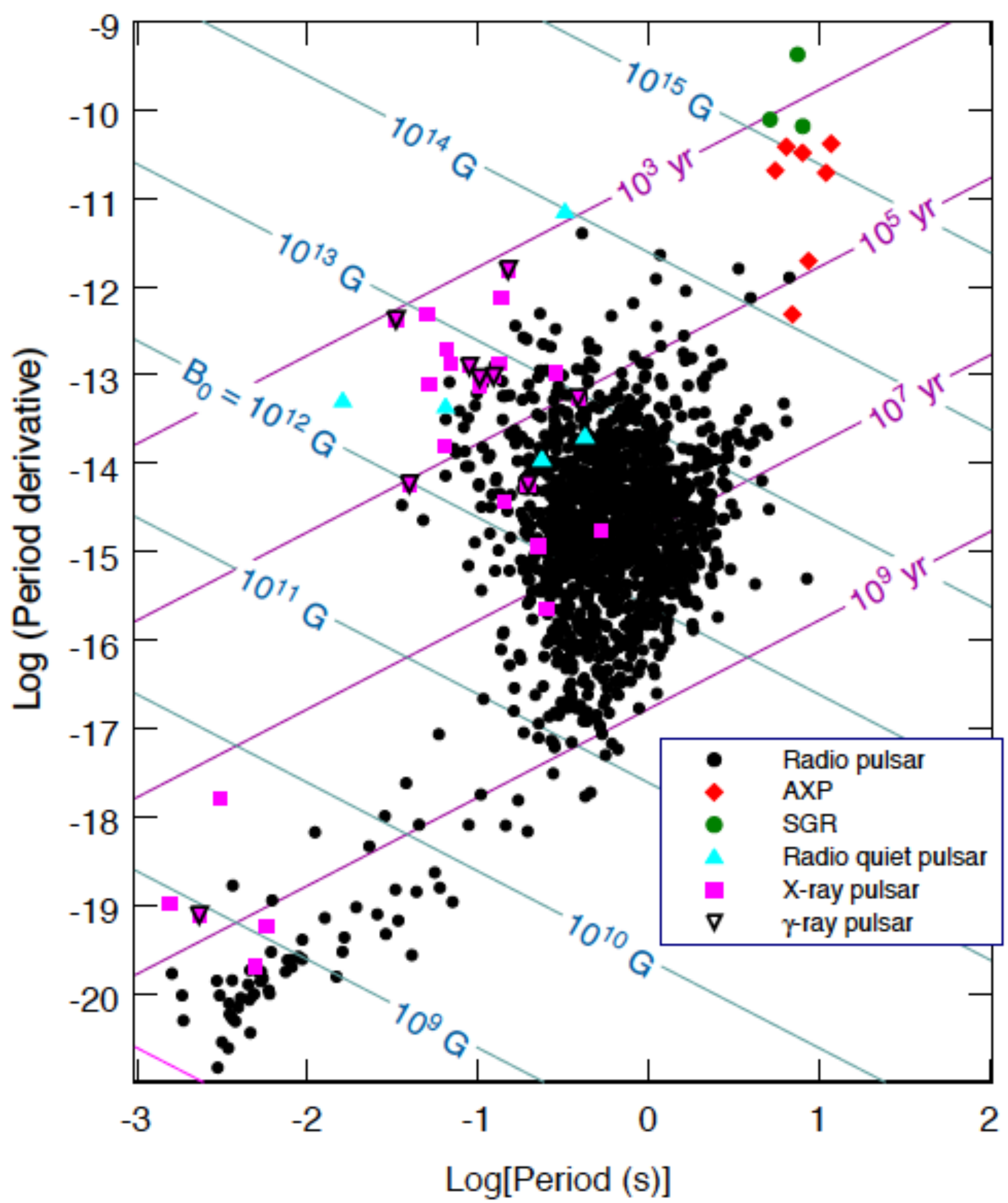

$$\dot{P}_{15} \equiv \dot{P}/(10^{-15}\,\mathrm{s\,s^{-1}})$$

$$B_s = \left(\frac{3Ic^3 P\dot{P}}{2\pi^2 R^6}\right)^{1/2} \simeq 2 \times 10^{12}\mathrm{G}\,(P\dot{P}_{15})^{1/2}$$

What if neutron star has a companion?

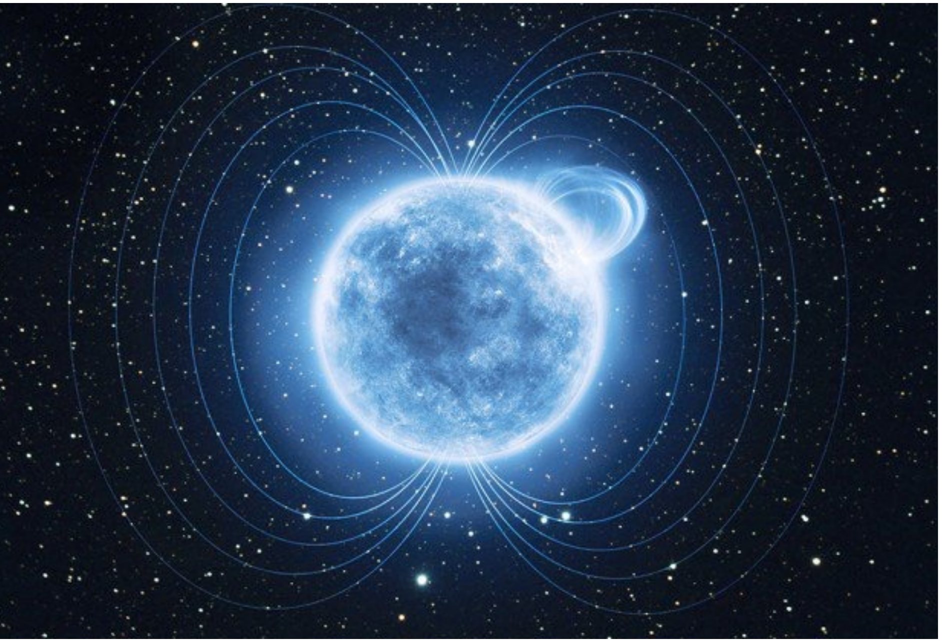

Some neutron stars are isolated and dim

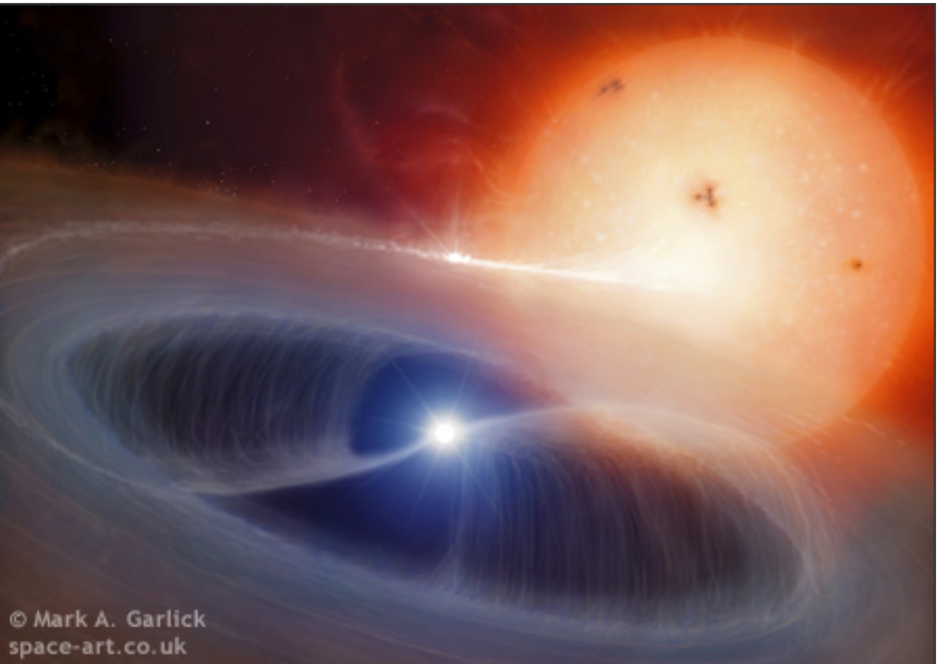

If neutron star has a close companion,
it absorbs material
and
can be extremely bright.

What if neutron star has a companion?

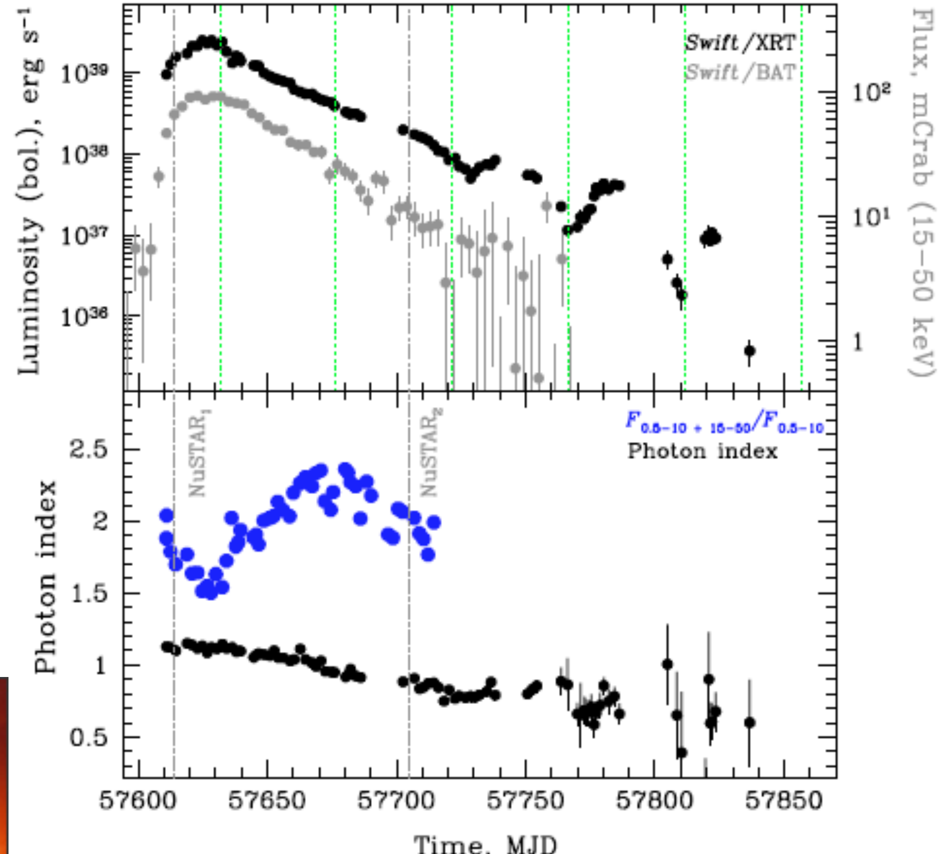

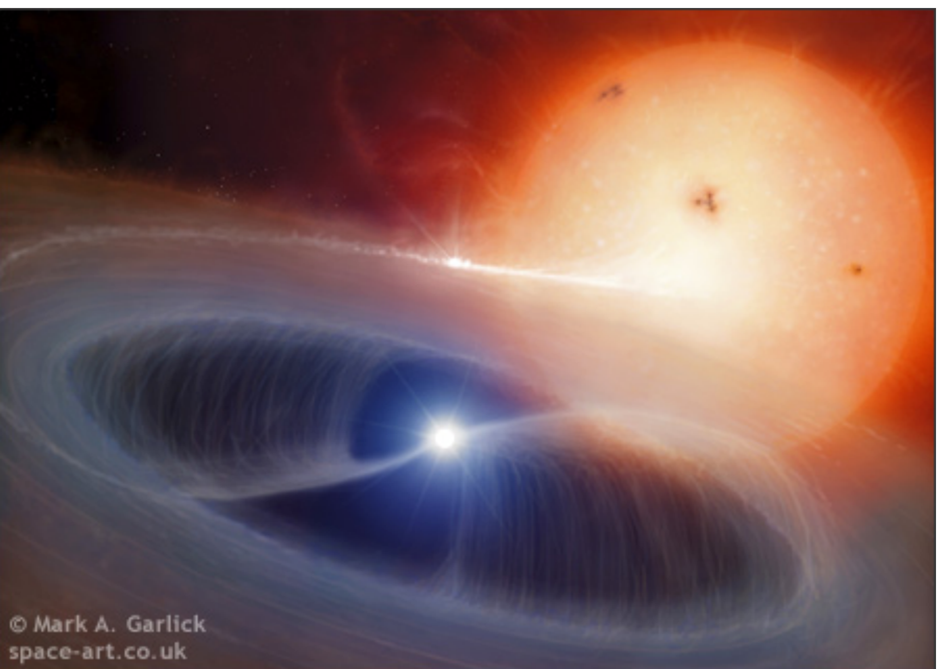

If neutron star has a close companion,
it absorbs material
and
can be extremely bright.

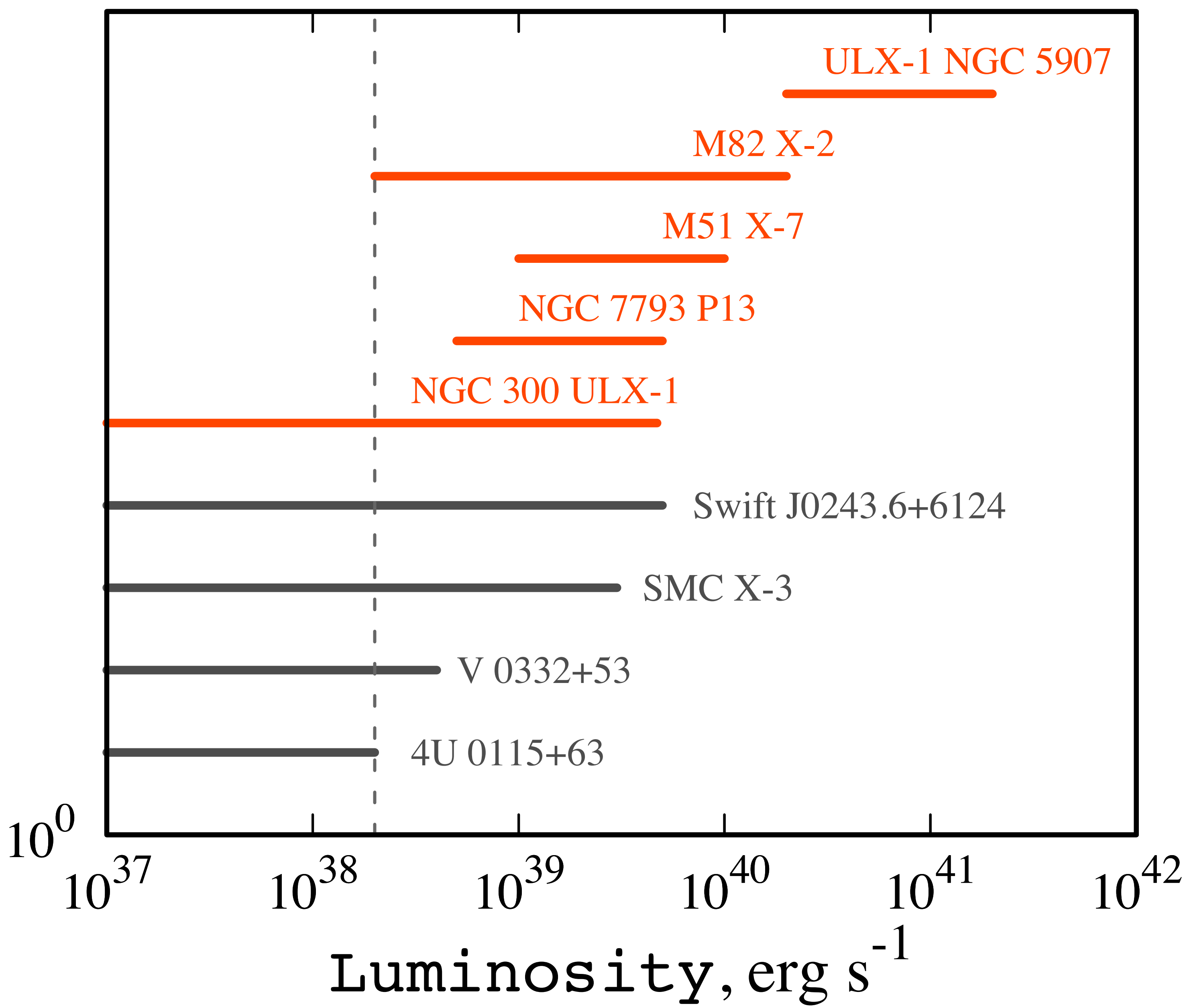

ULX-1 NGC 5907
M82 X-2
M51 X-7
NGC 7793 P13
NGC 300 ULX-1
Swift J0243.6+6124
SMC X-3
V 0332+53
4U 0115+63
10^0
10^37
10^38
10^39
10^40
10^41
10^42
Luminosity, erg s^-1

X-ray pulsar

Accretion Disc and its Interaction with B-field

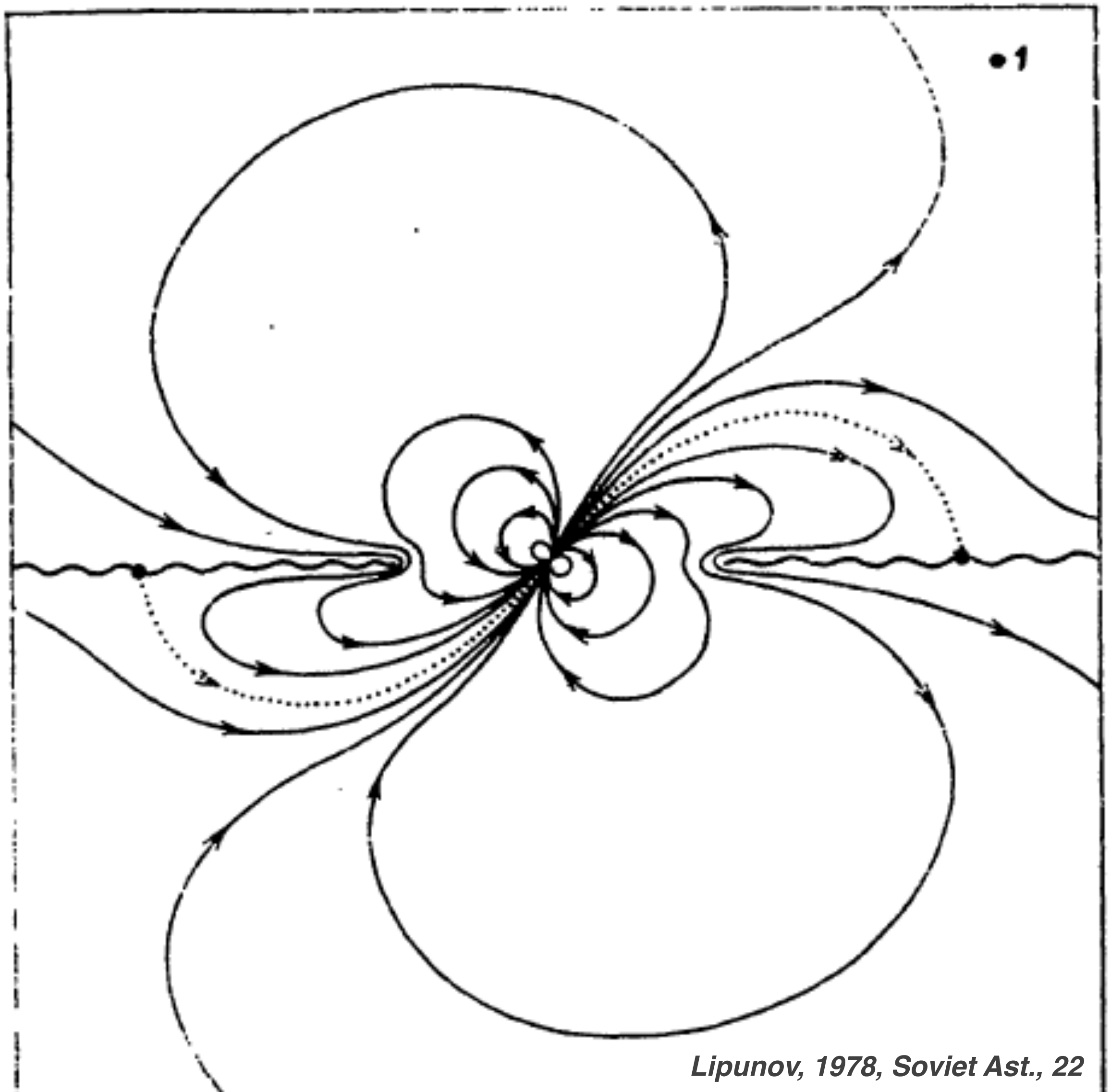

Lipunov, 1978, Soviet Ast., 22

The inner disc radius:

$$r_{\rm A} = \left(\frac{\mu^4}{2GM\dot{M}^2} \right)^{1/7}$$

$$r_{\rm m} = \xi r_{\rm A}$$

Co-rotational radius:

$$r_{\rm co} = \left(\frac{GM}{\Omega^2} \right)^{1/3}$$

Keplerian and stellar-rotation frequencies are equal

“Propeller” state

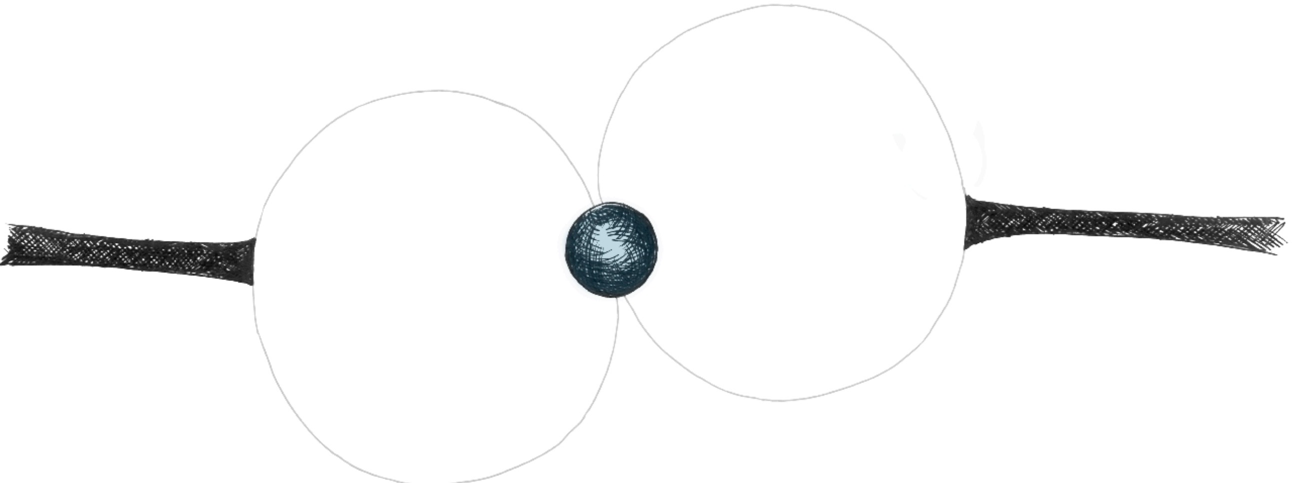

$r_m > r_{co}$

accretion is prohibited due to centrifugal barrier

Accretion state

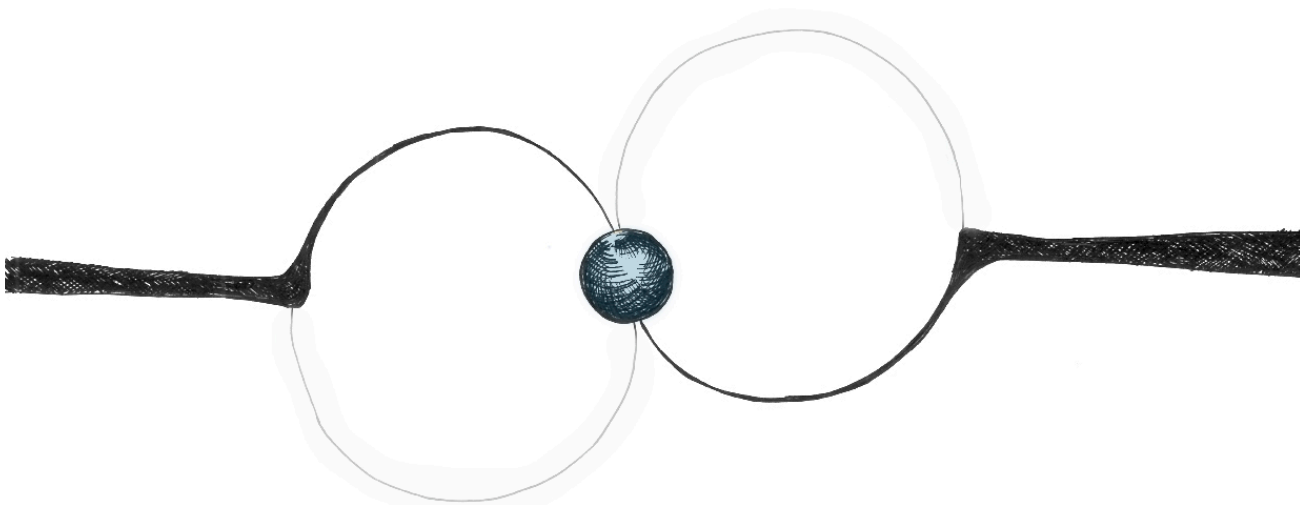

$r_m < r_{co}$

accretion is possible

Illarionov & Sunyaev, 1975

"Propeller" effect

Detection

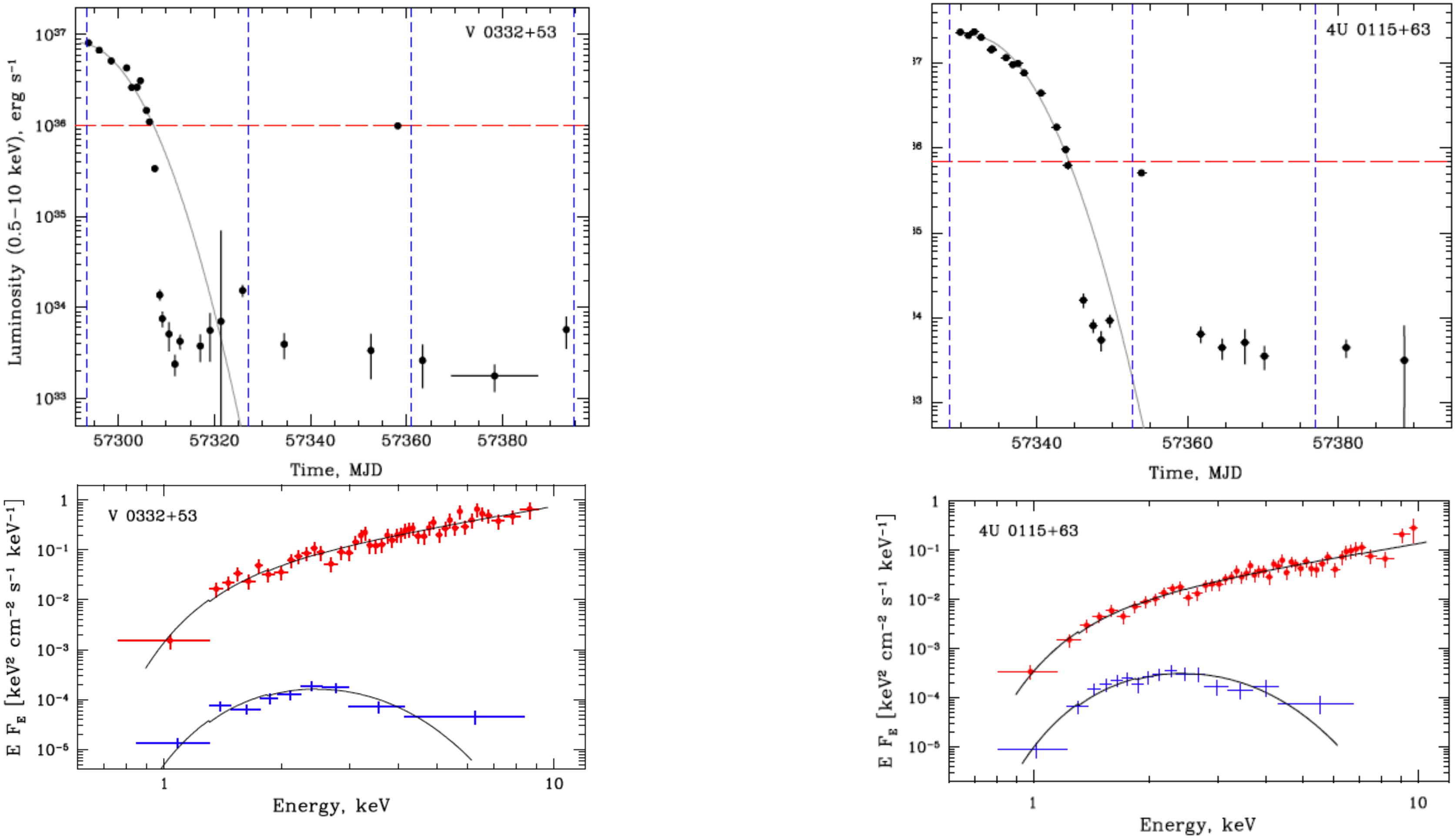

Tsygankov + 2016, A&A, 593

Propeller luminosity:

$$L_{\rm prop} \approx 3.5\times10^{36} B_{12}^2 P^{-7/3} M_{1.4}^{-2/3} R_6^5 \ \text{erg s}^{-1}$$

“Propeller” effect

Detection

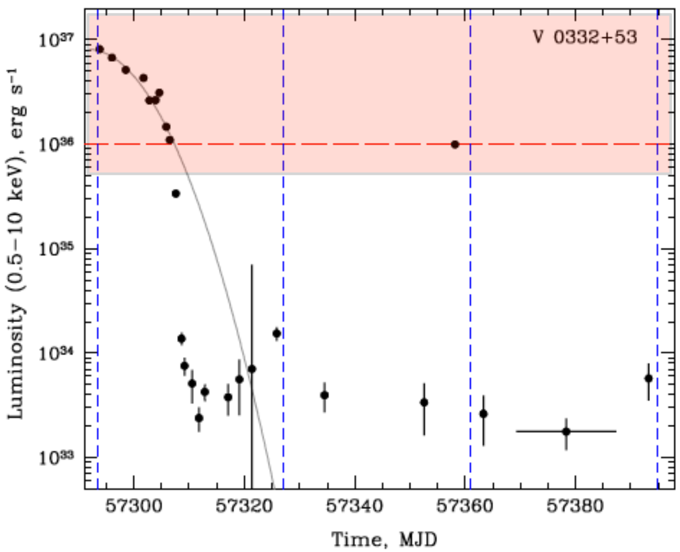

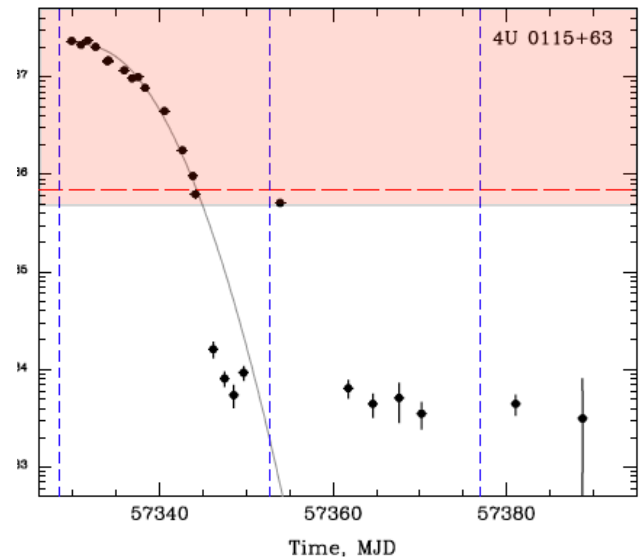

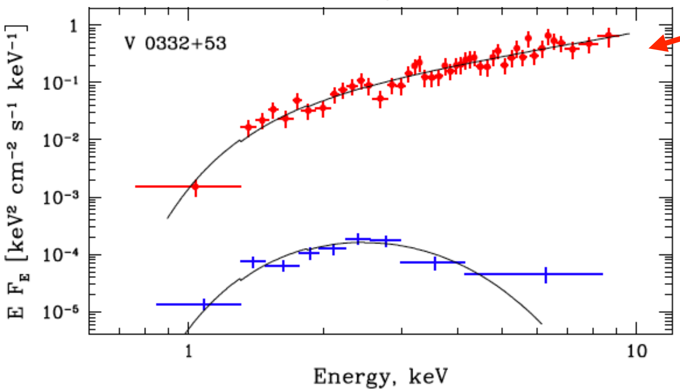

Absorbed power-law

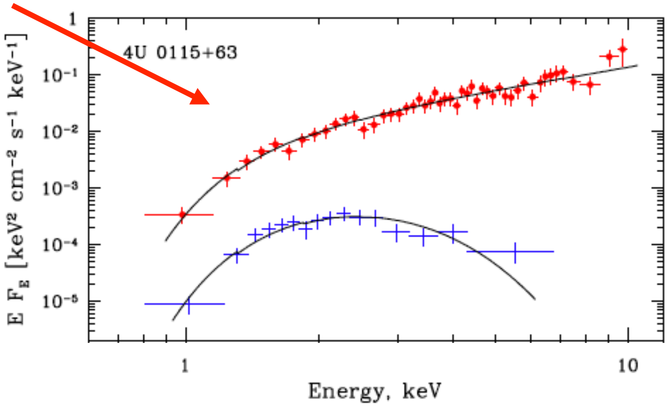

Tsygankov + 2016, A&A, 593

Propeller luminosity:

$$L_{\rm prop} \approx 3.5\times10^{36} B_{12}^{2} P^{-7/3} M_{1.4}^{-2/3} R_{6}^{5}\ \ {\rm erg\ s^{-1}}$$

"Propeller" effect

Detection

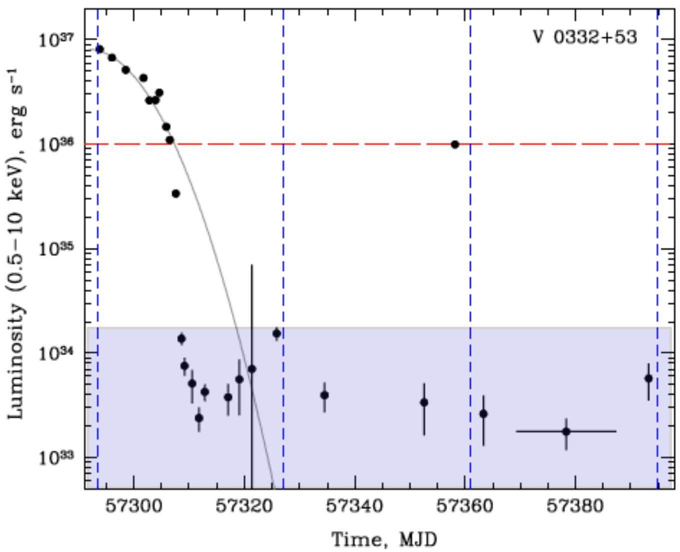

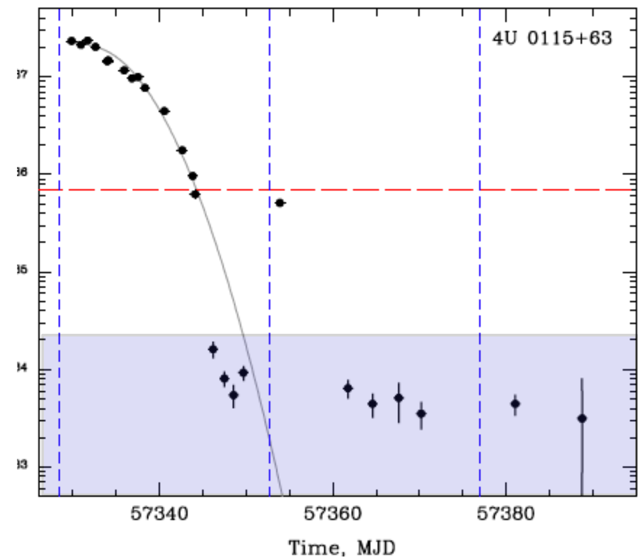

Tsygankov + 2016, A&A, 593

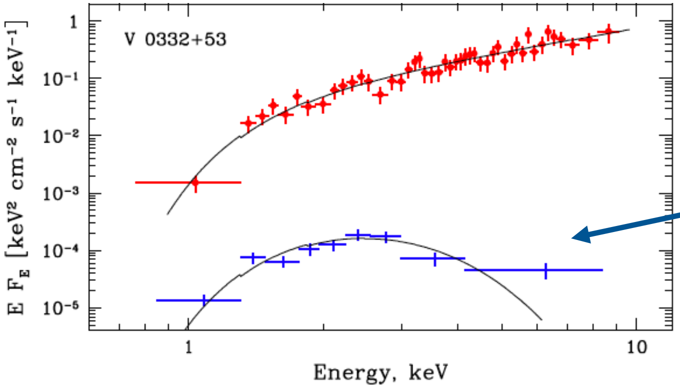

Black body with T=0.5 keV

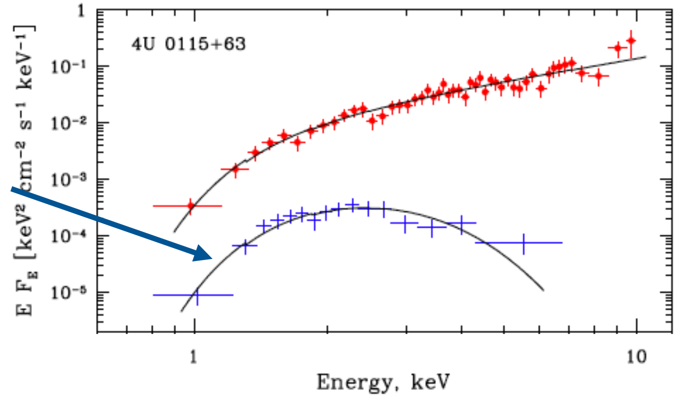

Propeller luminosity:

$$L_{\rm prop} \approx 3.5\times10^{36} B_{12}^2 P^{-7/3} M_{1.4}^{-2/3} R_6^5 \ \ {\rm erg\ s^{-1}}$$

X-ray pulsars: pulse profiles

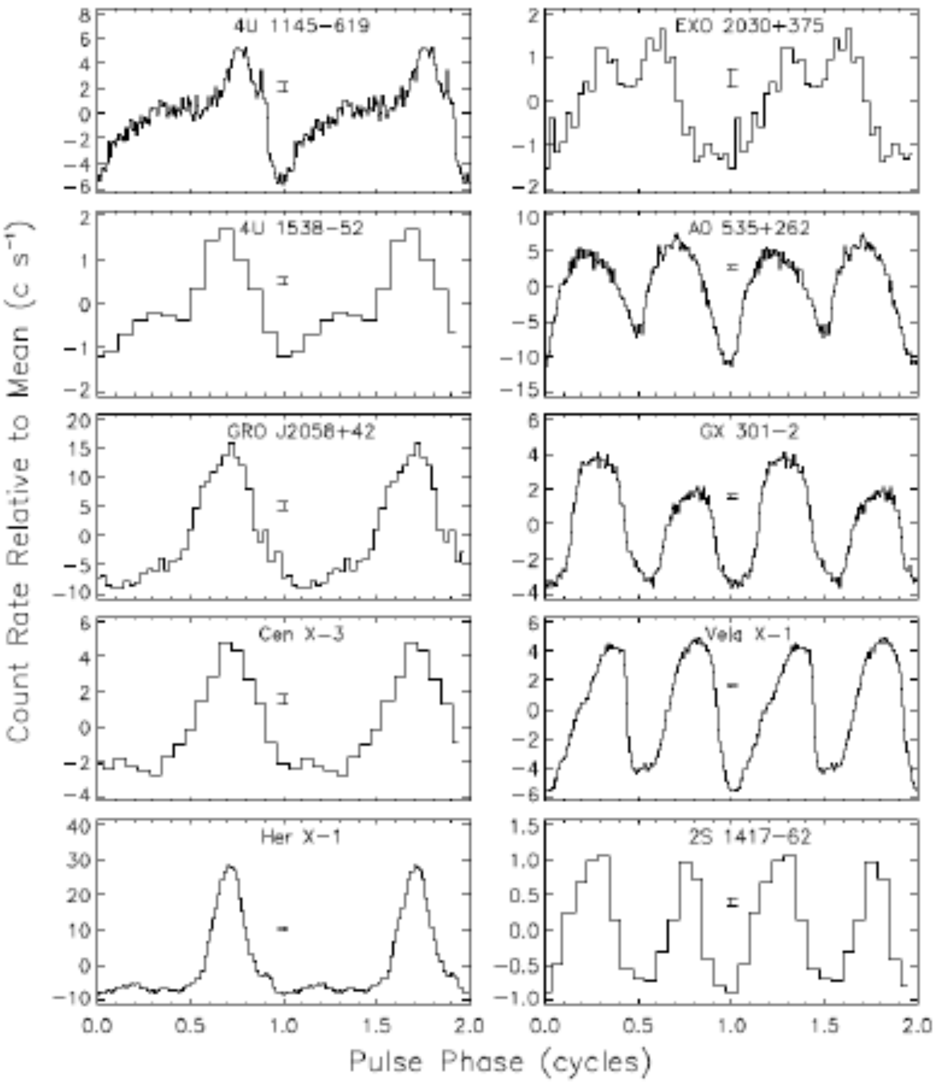

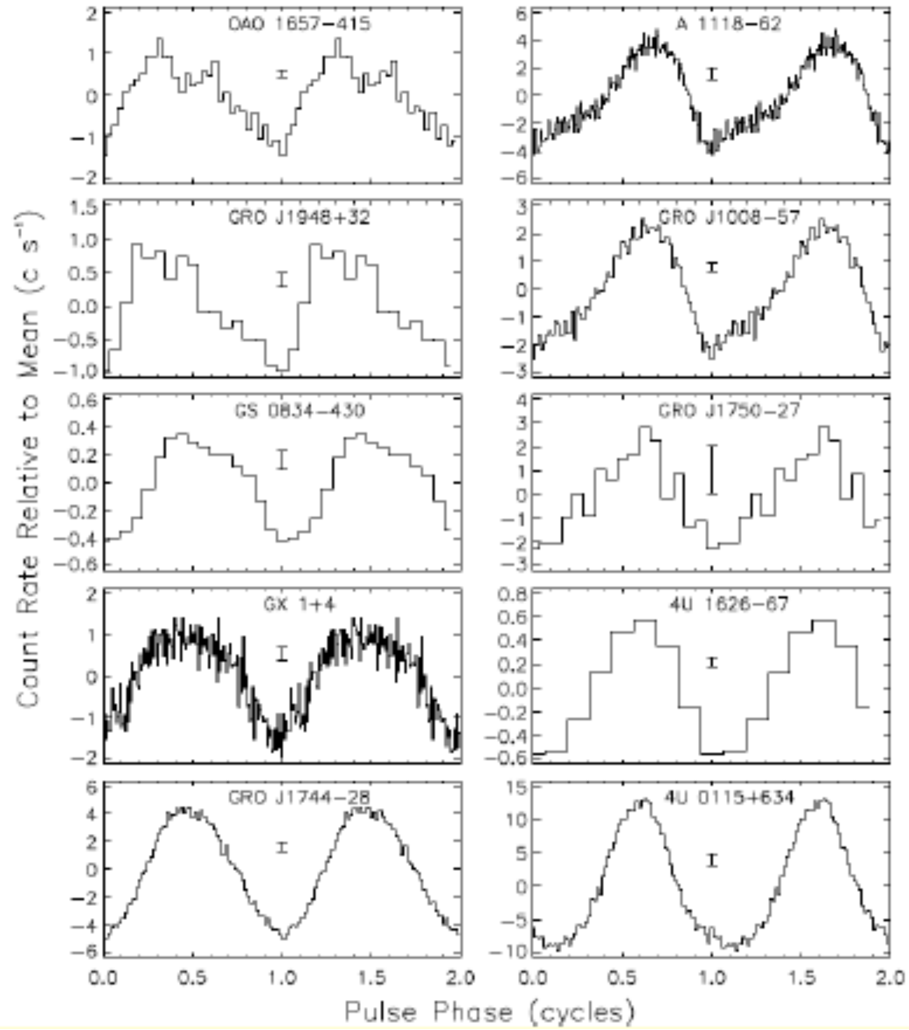

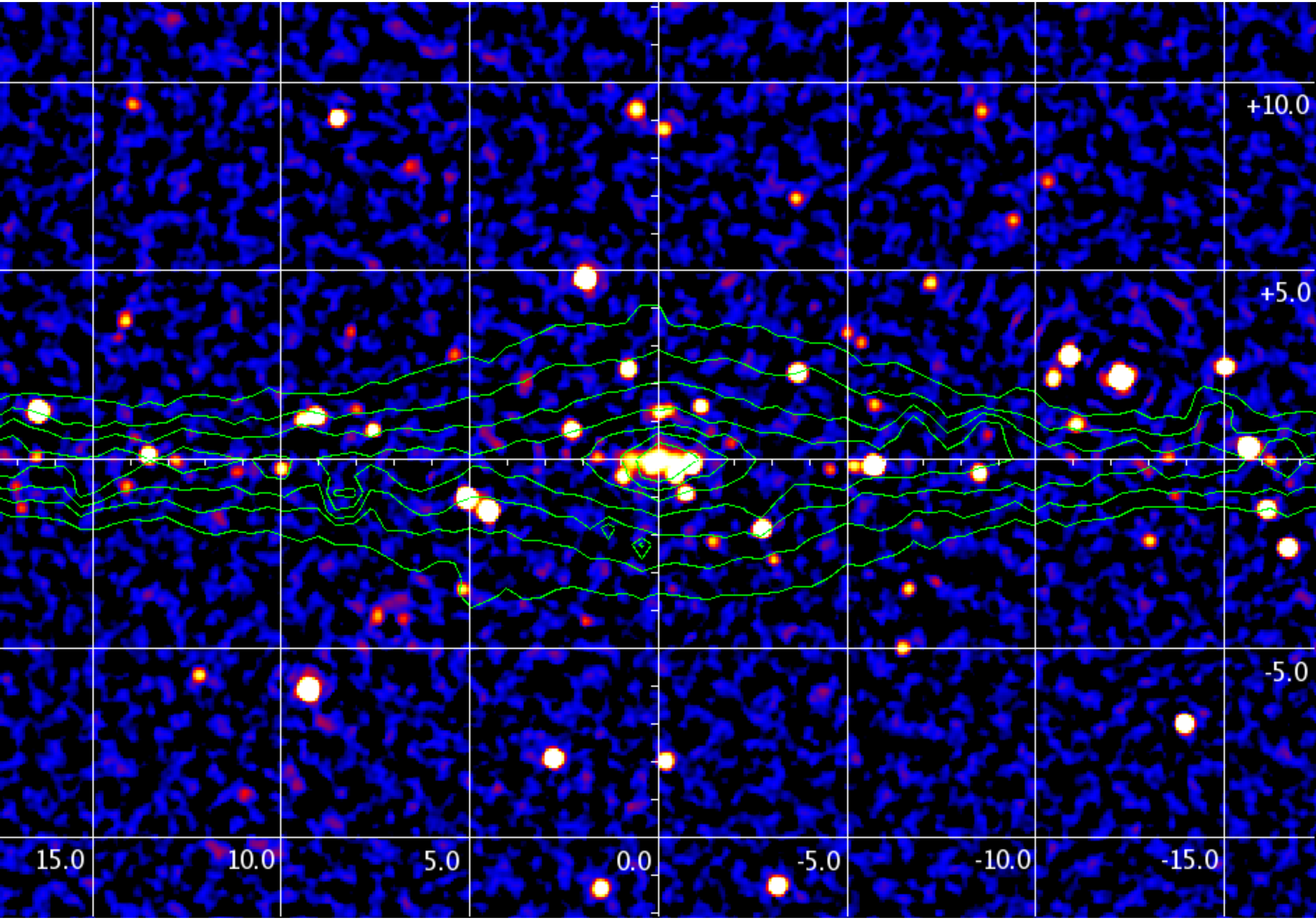

Krivonos+, 2012, A&A, 545

Magnetic field strengths

Magnetic field strengths

Magnetic field strengths

Earth — 1

Stars — 10^3

Strongest field in lab — 10^6

G

Magnetic field strengths

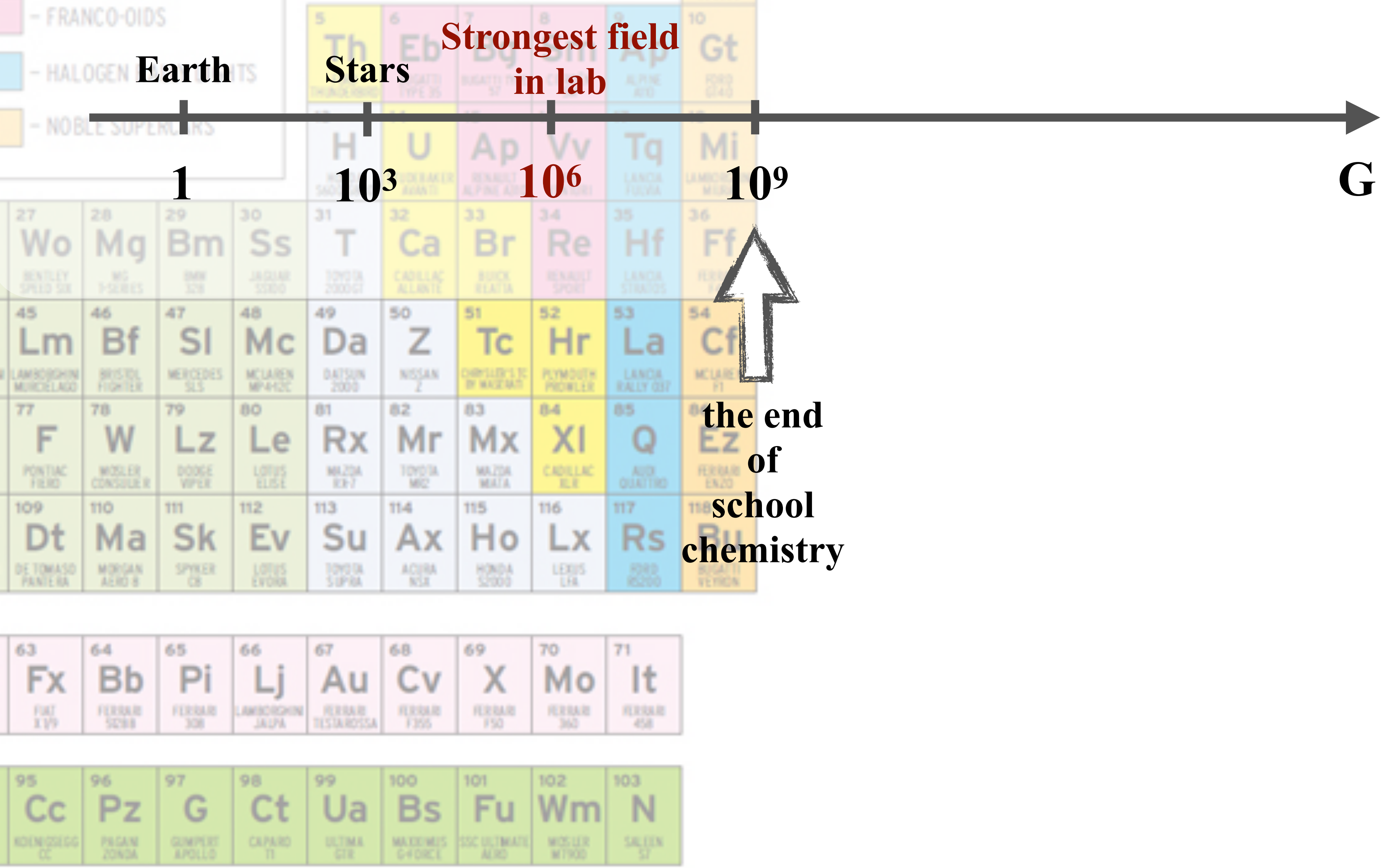

Magnetic field strengths

Earth	Stars	Strongest field in lab		Young neutron stars	
1	10^3	10^6	10^9	10^{12-15}	G

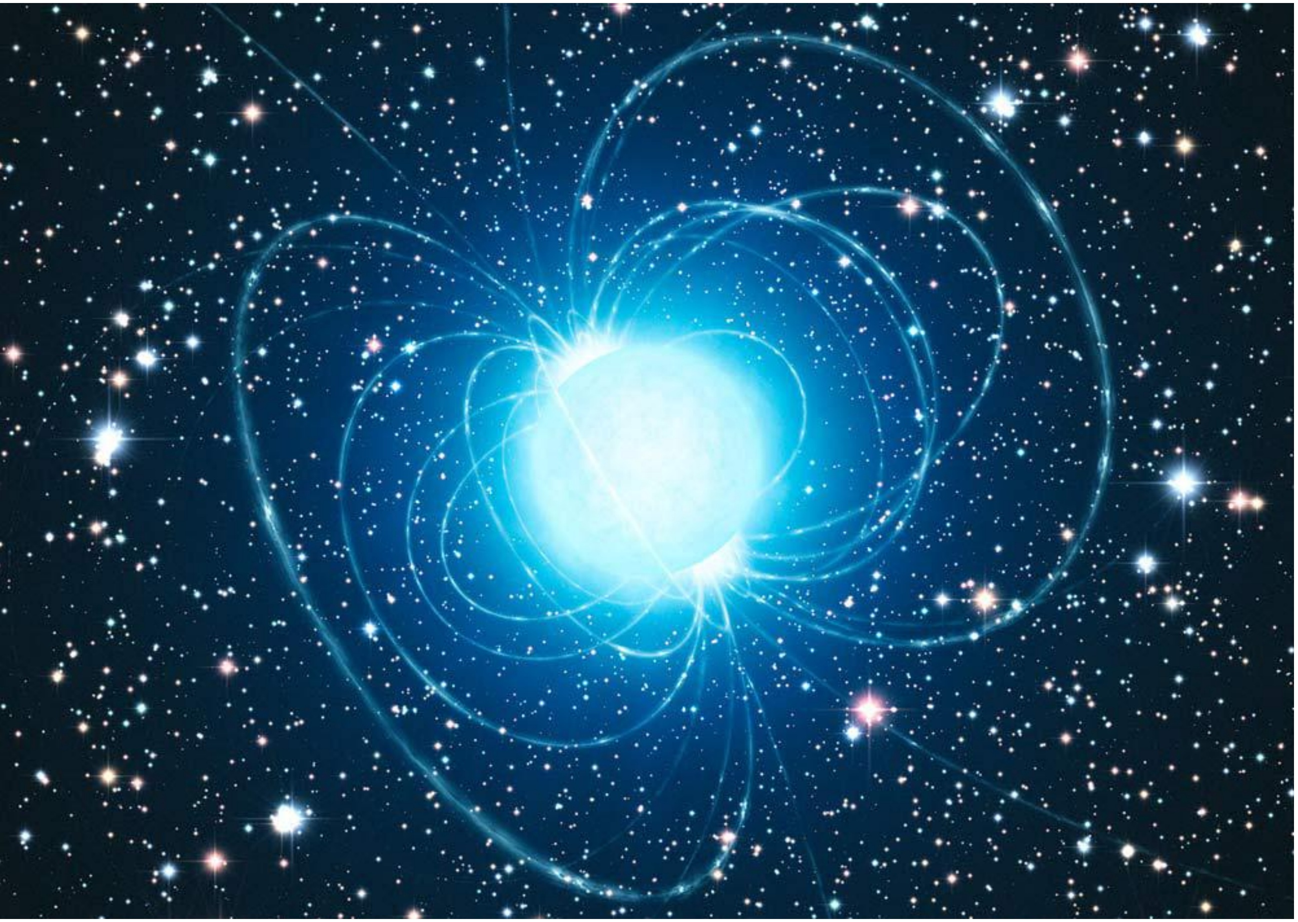

Extreme physics

Deviations from Quantum Electrodynamics?

Compton scattering: non-magnetic case

$$\sigma_{\mathrm{T}} = \frac{8\pi}{3}\left(\frac{e^2}{m_{\mathrm{e}}c^2}\right)^2 \approx 6.65 \times 10^{-25}\,\mathrm{cm}^2$$

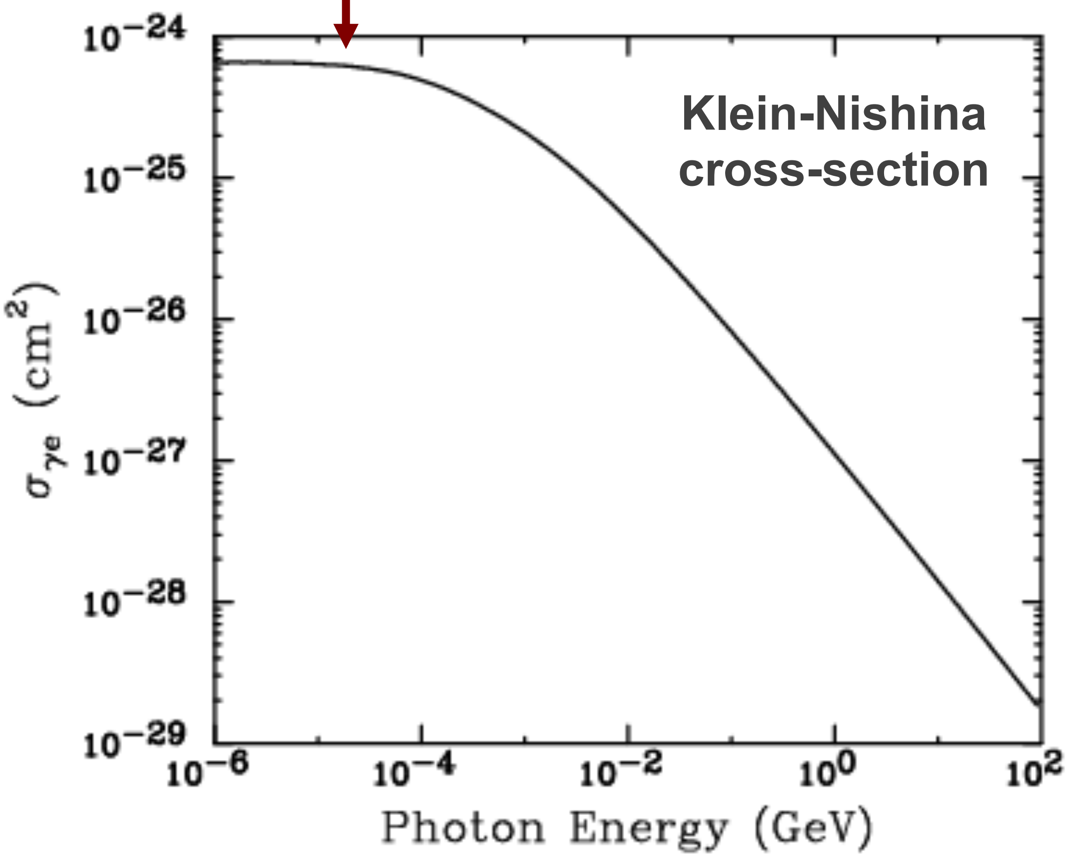

Compton scattering: non-magnetic case

$$\sigma_{\mathrm{T}} = \frac{8\pi}{3}\left(\frac{e^2}{m_{\mathrm{e}}c^2}\right)^2 \approx 6.65 \times 10^{-25}\,\mathrm{cm}^2$$

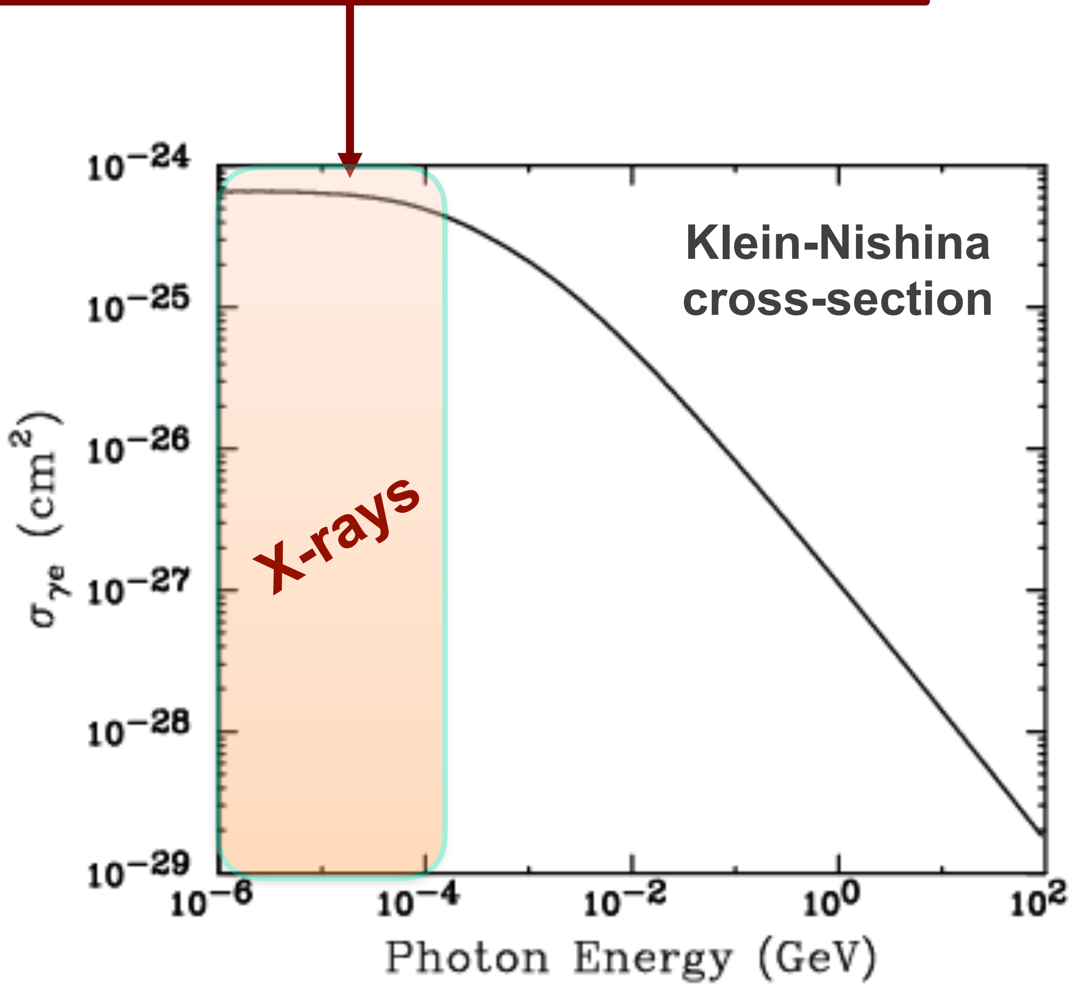

X-ray pulsar

Typical spectra

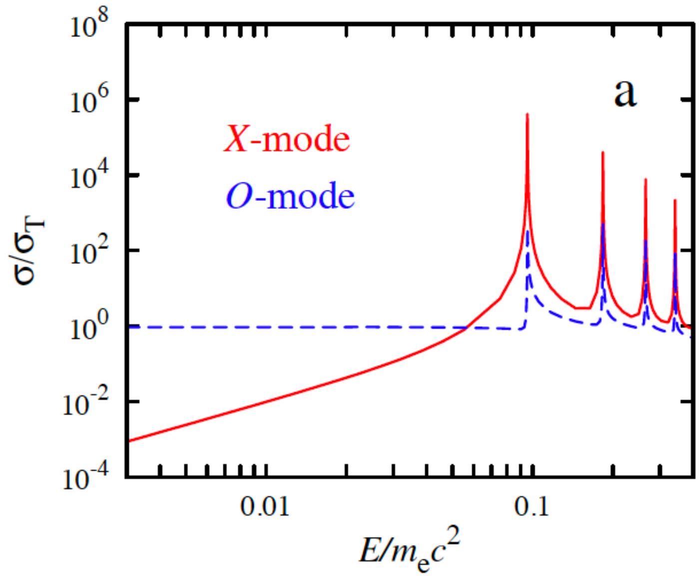

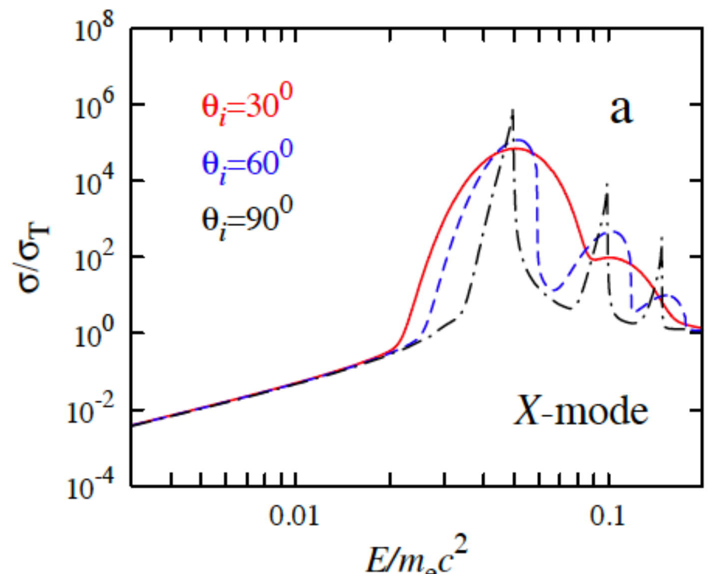

AM+, 2016, Ph.Rev.D

Spectra of V 0332+53 at different luminosity states

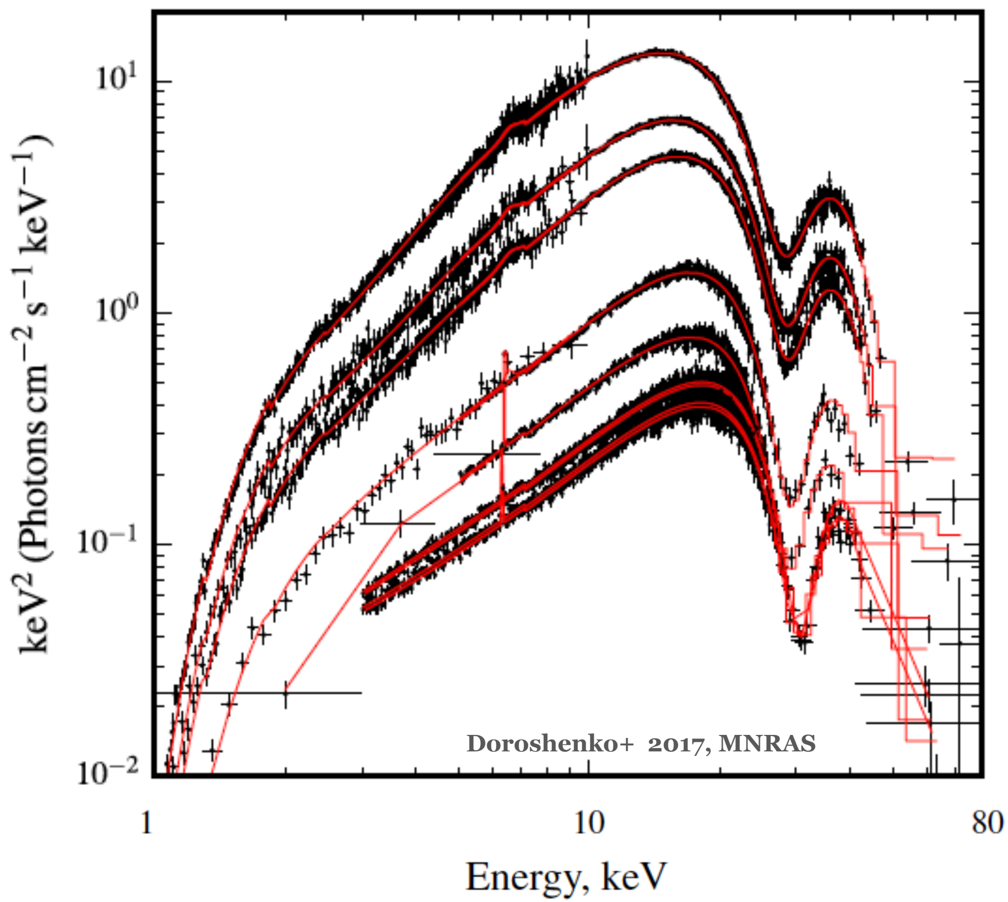

$$E_{cyc} = 11.6\, B_{12}\, \mathrm{keV}$$

X-ray pulsar

Typical spectra

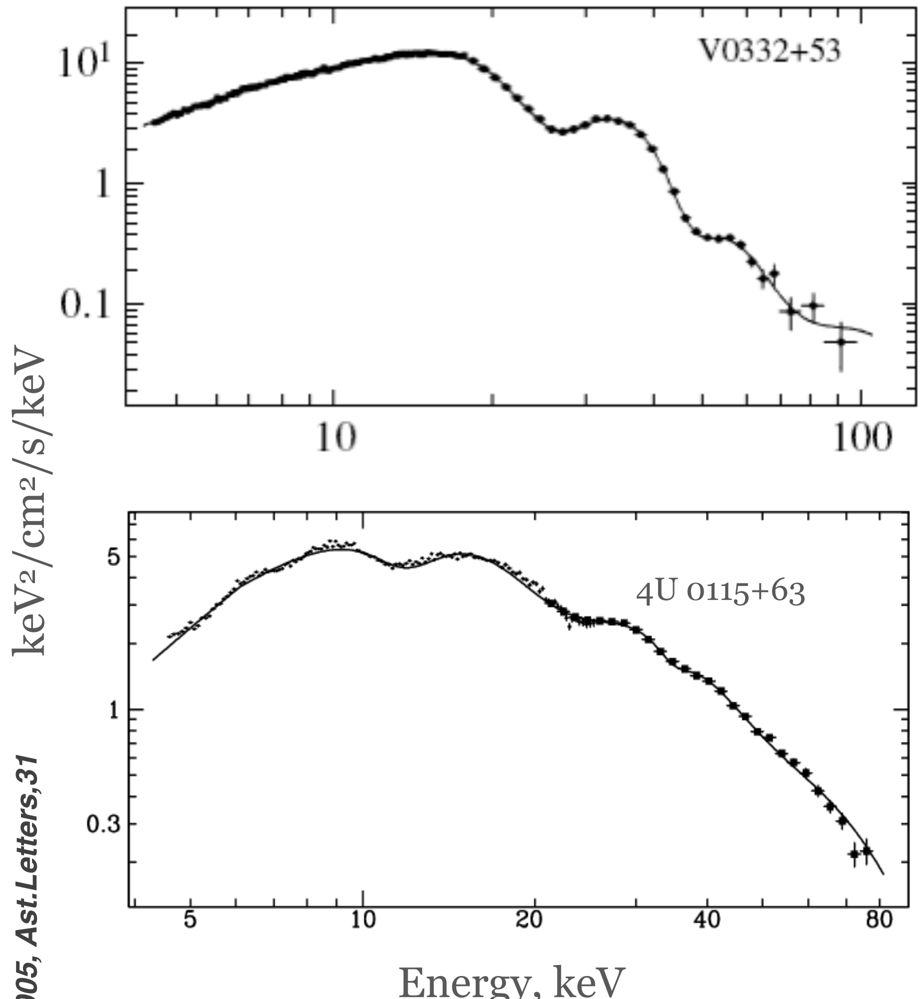

Filippova+, 2005, Ast.Letters,31

$$E_{\mathrm{cyc}} = 11.6\, B_{12}\, \mathrm{keV}$$

Source name	Cyclotron energy, keV
4U 0115+63 (–)	11.5, 20.1, 33.6, 49.5, 53
V 0332+53 (–)	28, 53, 74
4U 0352+309 (X Per)	29
RX J0440.9+4431	32
RX J0520.5-6932	31.5
A 0535+262	50, 110
MXB 0656–072	36
Vela X-1 (+)	27,54
GRO J1008-57	88?, 75.5
1A 1118–61	55
Cen X-3	28
GX 301–2	37, 48
GX 304–1 (+)	50.8
4U 1538–52	20, 47
Swift J1626.6–5156	10
4U 1626–67	37
Her X-1 (+)	42
OAO 1657–415	36
GRO J1744–28	4.7
IGR J18179–1621	21
GS 1843+00	20
4U 1907+09	19, 40
4U 1909+07	44?
XTE J1946+274	36
KS 1947+300	12.5
EXO 2030+375	11?, 36?, 63?
Cep X-4	30

X-ray pulsar

Typical spectra

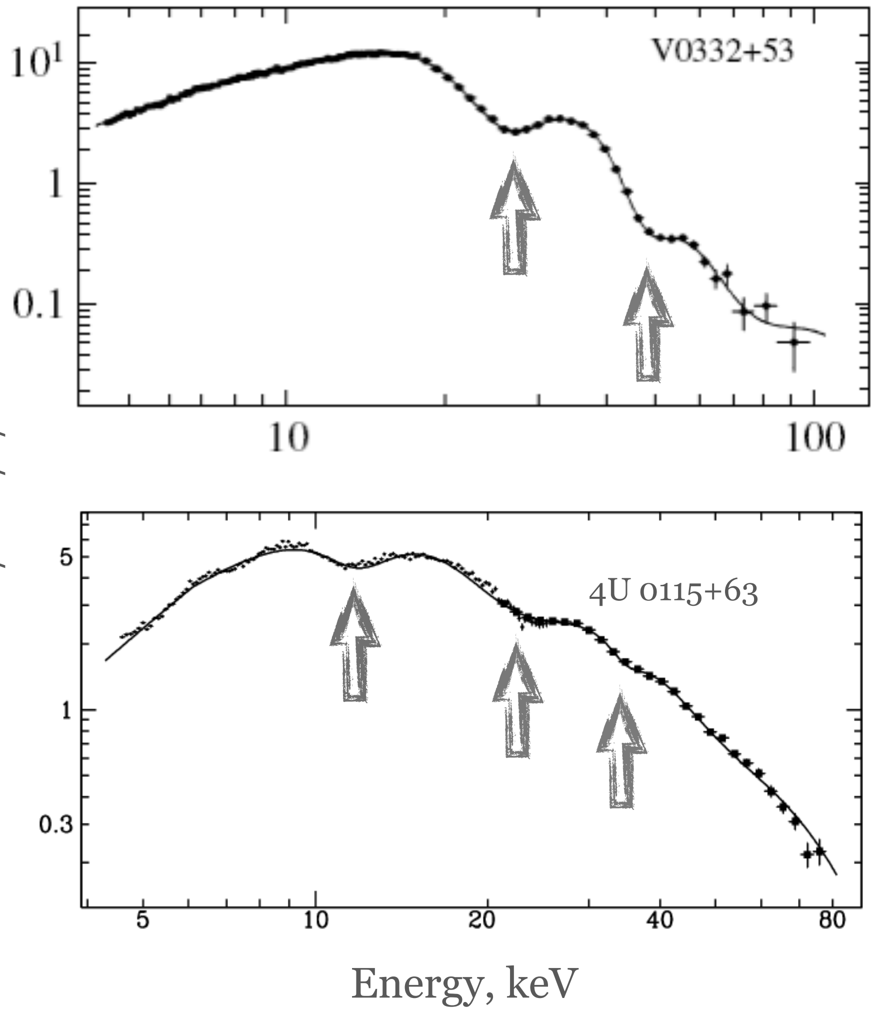

Filippova+, 2005, Ast.Letters,31

$$E_{\rm cyc} = 11.6\, B_{12}\, {\rm keV}$$

Source name	Cyclotron energy, keV
4U 0115+63 (–)	11.5, 20.1, 33.6, 49.5, 53
V 0332+53 (–)	28, 53, 74
4U 0352+309 (X Per)	29
RX J0440.9+4431	32
RX J0520.5-6932	31.5
A 0535+262	50, 110
MXB 0656–072	36
Vela X-1 (+)	27,54
GRO J1008-57	$88^?$, 75.5
1A 1118–61	55
Cen X-3	28
GX 301–2	37, 48
GX 304–1 (+)	50.8
4U 1538–52	20, 47
Swift J1626.6–5156	10
4U 1626–67	37
Her X-1 (+)	42
OAO 1657–415	36
GRO J1744–28	4.7
IGR J18179–1621	21
GS 1843+00	20
4U 1907+09	19, 40
4U 1909+07	$44^?$
XTE J1946+274	36
KS 1947+300	12.5
EXO 2030+375	$11^?$, $36^?$, $63^?$
Cep X-4	30

High mass accretion rate

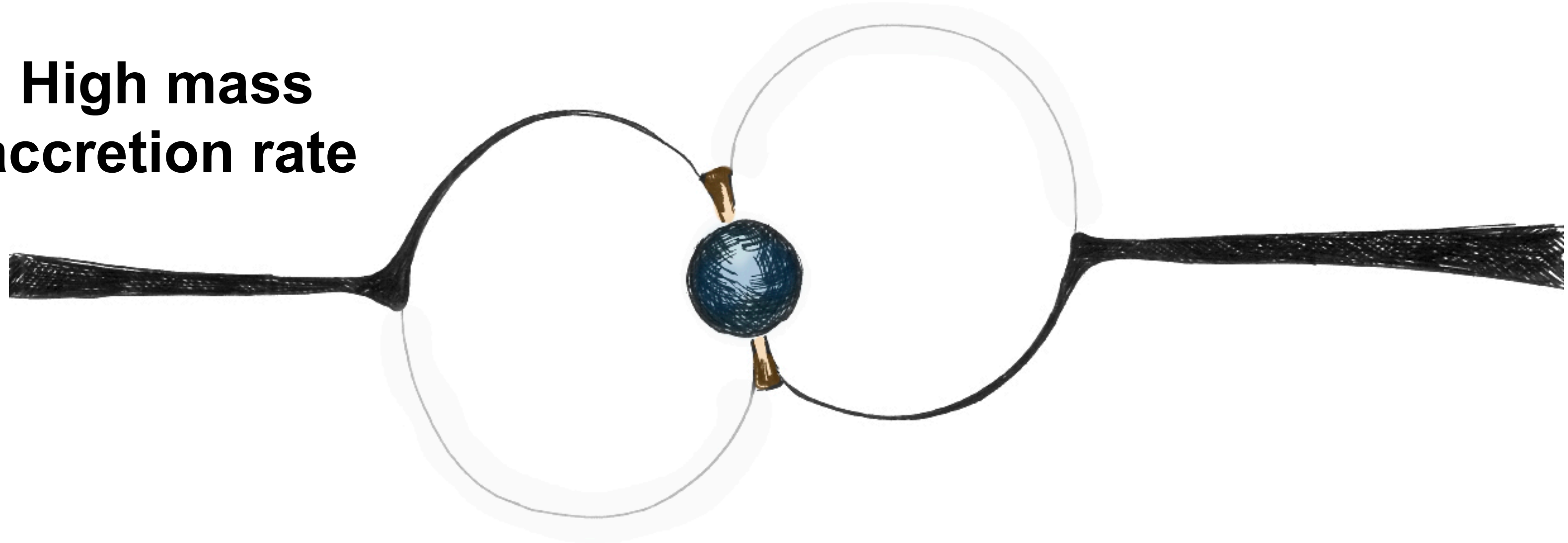

Critical luminosity

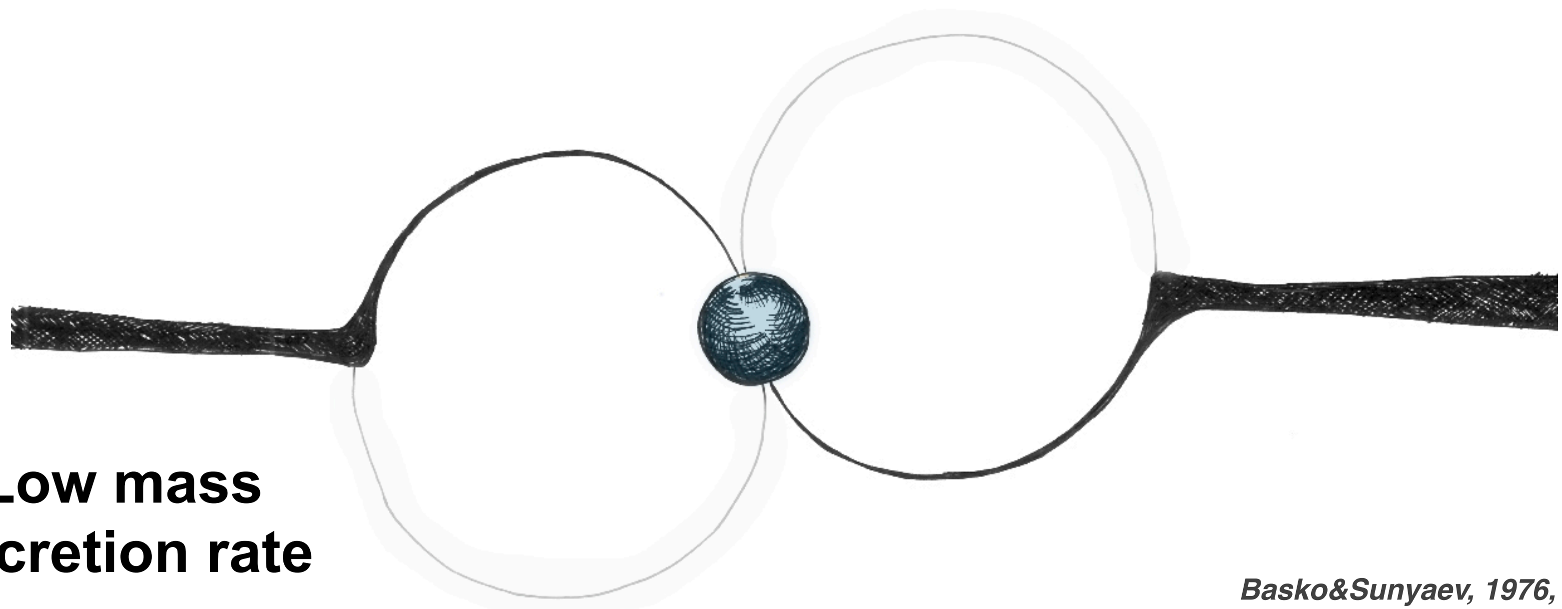

Low mass accretion rate

Basko&Sunyaev, 1976, MNRAS
AM+, 2015, MNRAS, 447

Critical luminosity

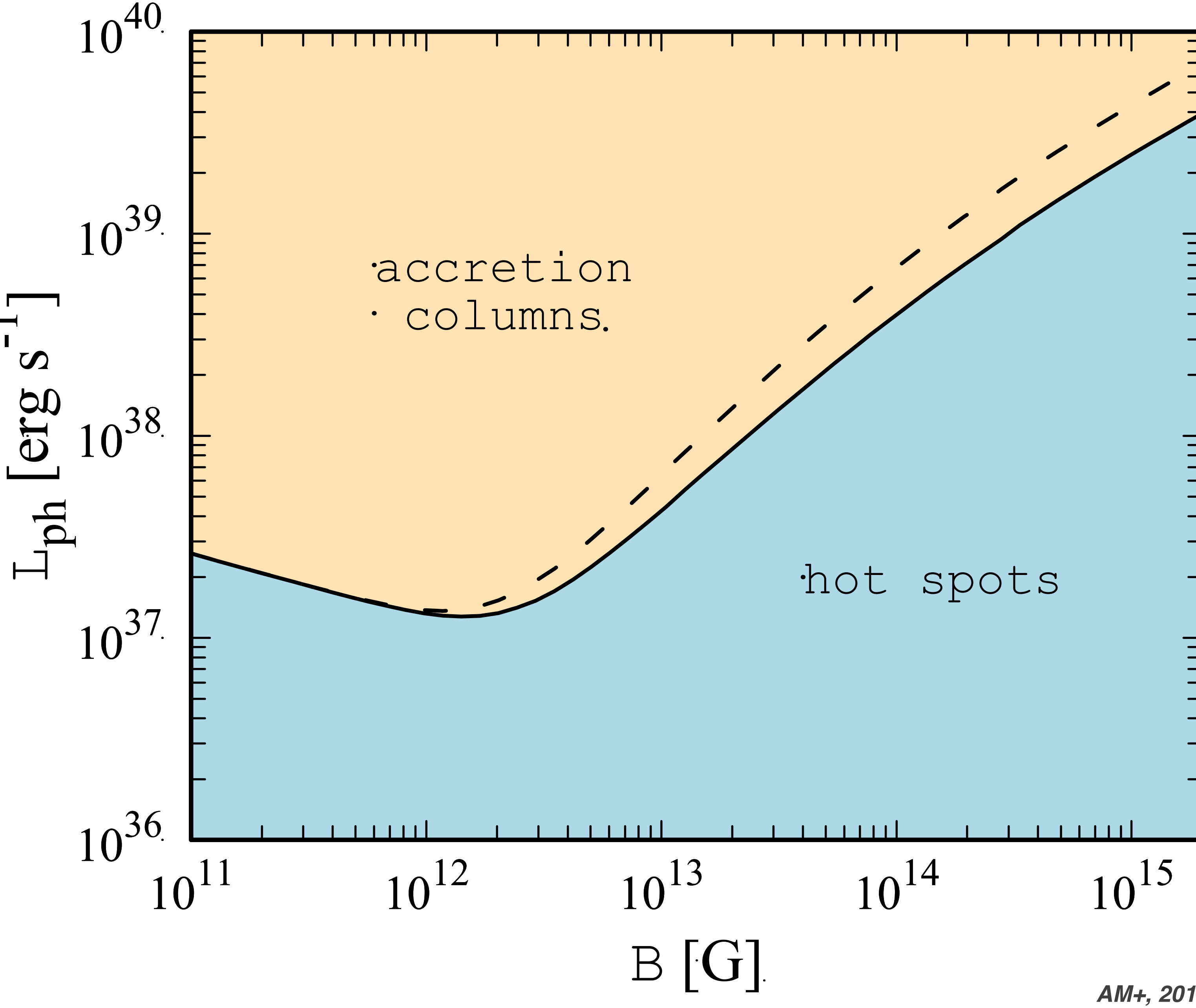

AM+, 2015, MNRAS, 447

Critical luminosity

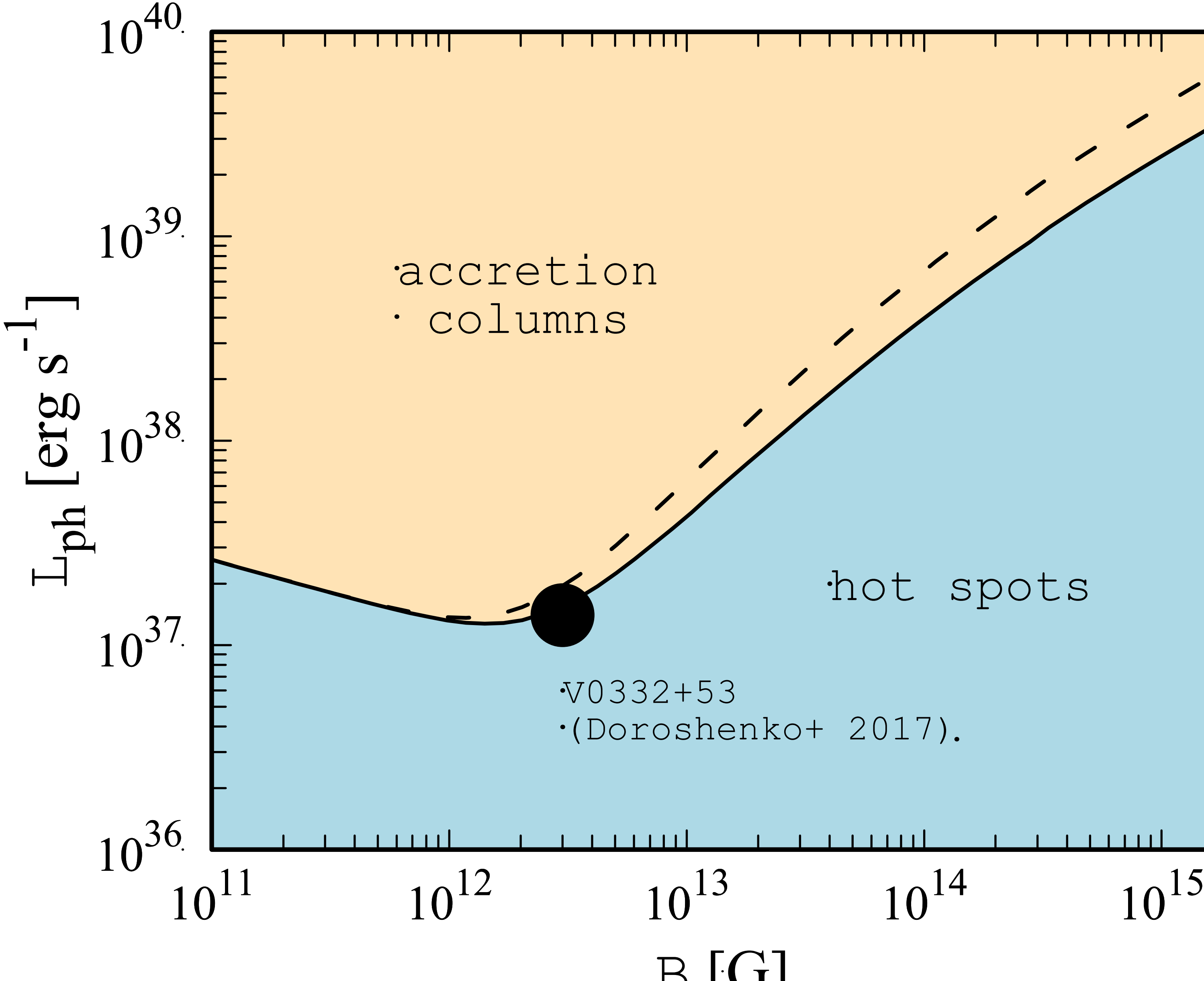

AM+, 2015, MNRAS, 447

Above the critical luminosity: accretion column

A set of assumptions:

(1) dipole magnetic field;
(2) geometrical thickness is determined by the thickness of accretion disc at the magnetospheric radius;
(3) accretion flow stops at radiation dominated shock and slowly settles in inside a sinking region
(4) the gravitational force will be offset by the radiation pressure gradient
(5) the gas pressure is unimportant

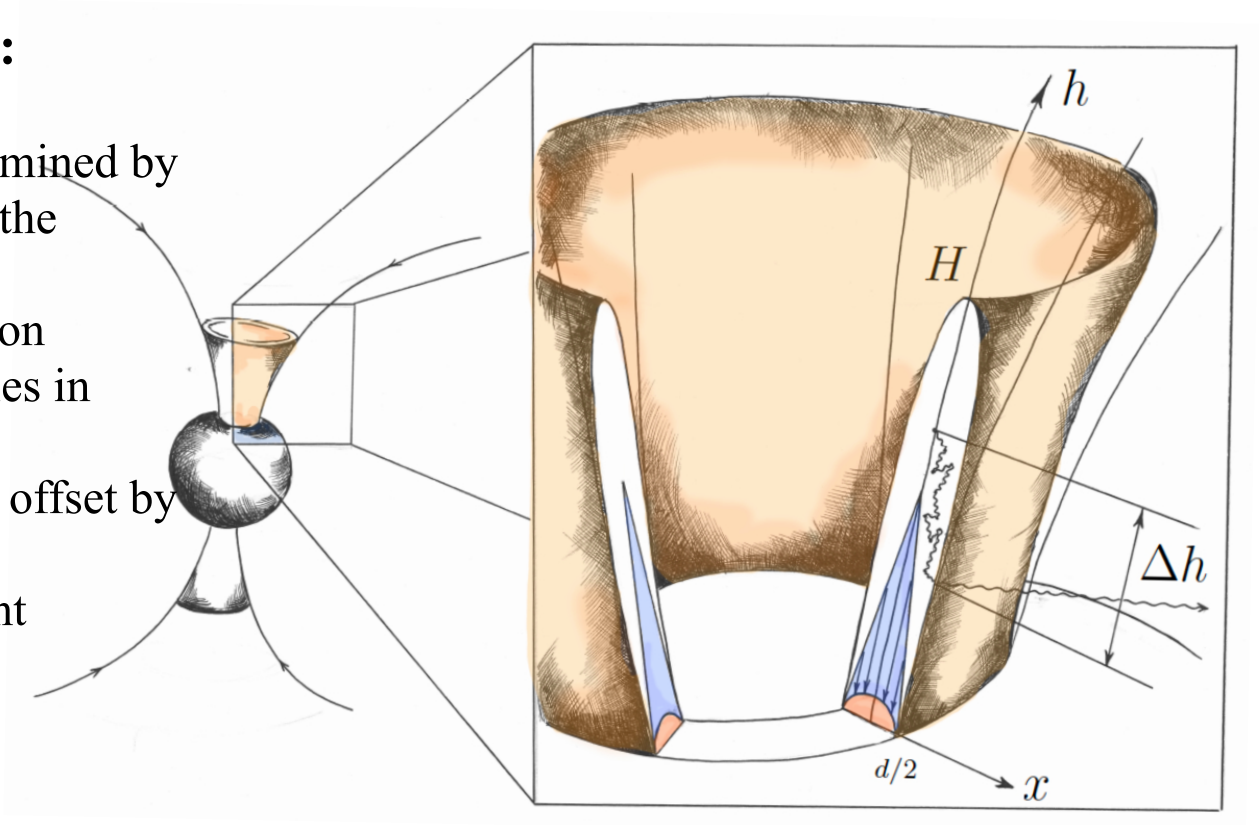

$$L(H = R) \approx 1.8 \times 10^{39} \left(\frac{l_0/d_0}{50}\right) \left(\frac{\kappa_T}{\kappa_\perp}\right) \frac{M}{M_\odot} \mathrm{erg\,s}^{-1}$$

AM+, 2015, MNRAS, 454, 2714

Stable accretion columns cannot be infinitely bright

The reason:

The higher the mass accretion rate
=> the higher the temperature
=> the higher photon energy
=> the higher the cross-sections

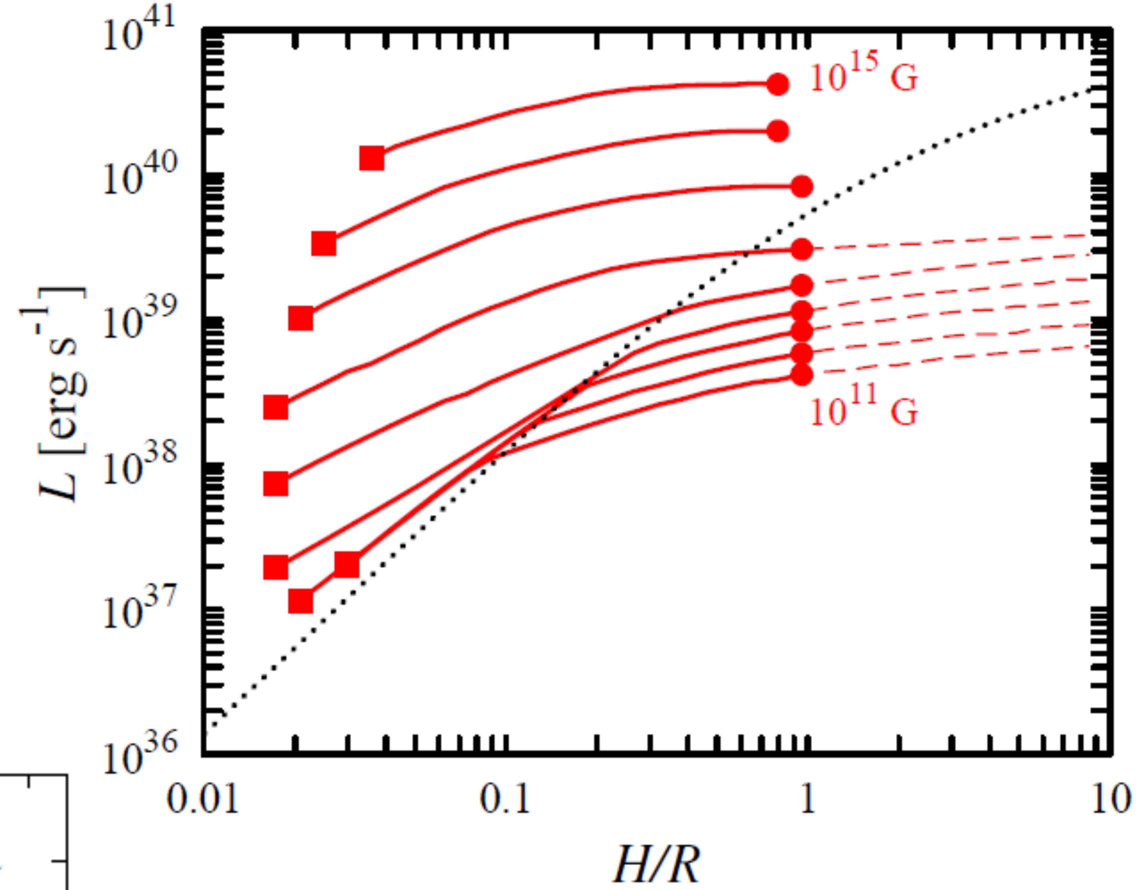

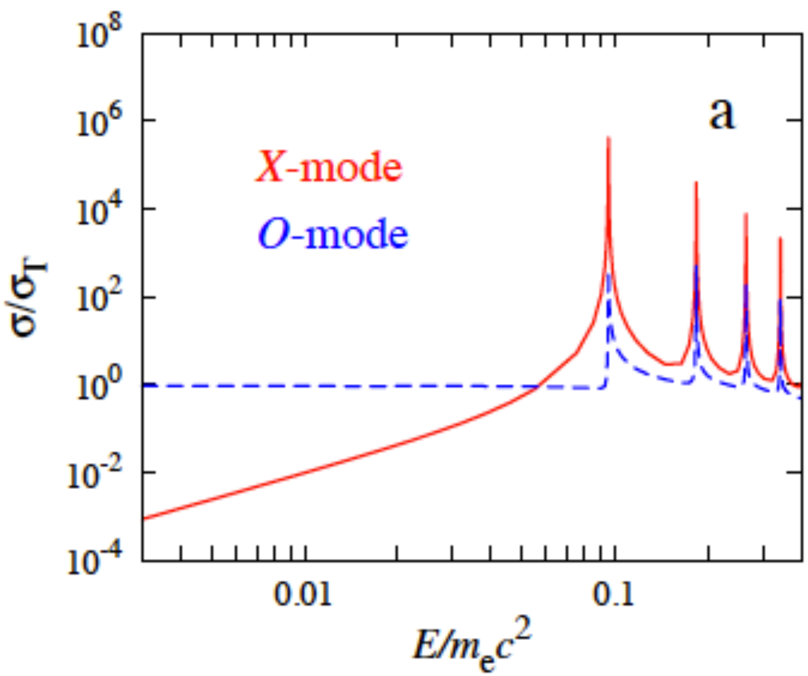

Basko & Sunyaev, 1976, MNRAS, 175
AM+, 2015, MNRAS, 454

Pulsations from ULX in M82: explanation

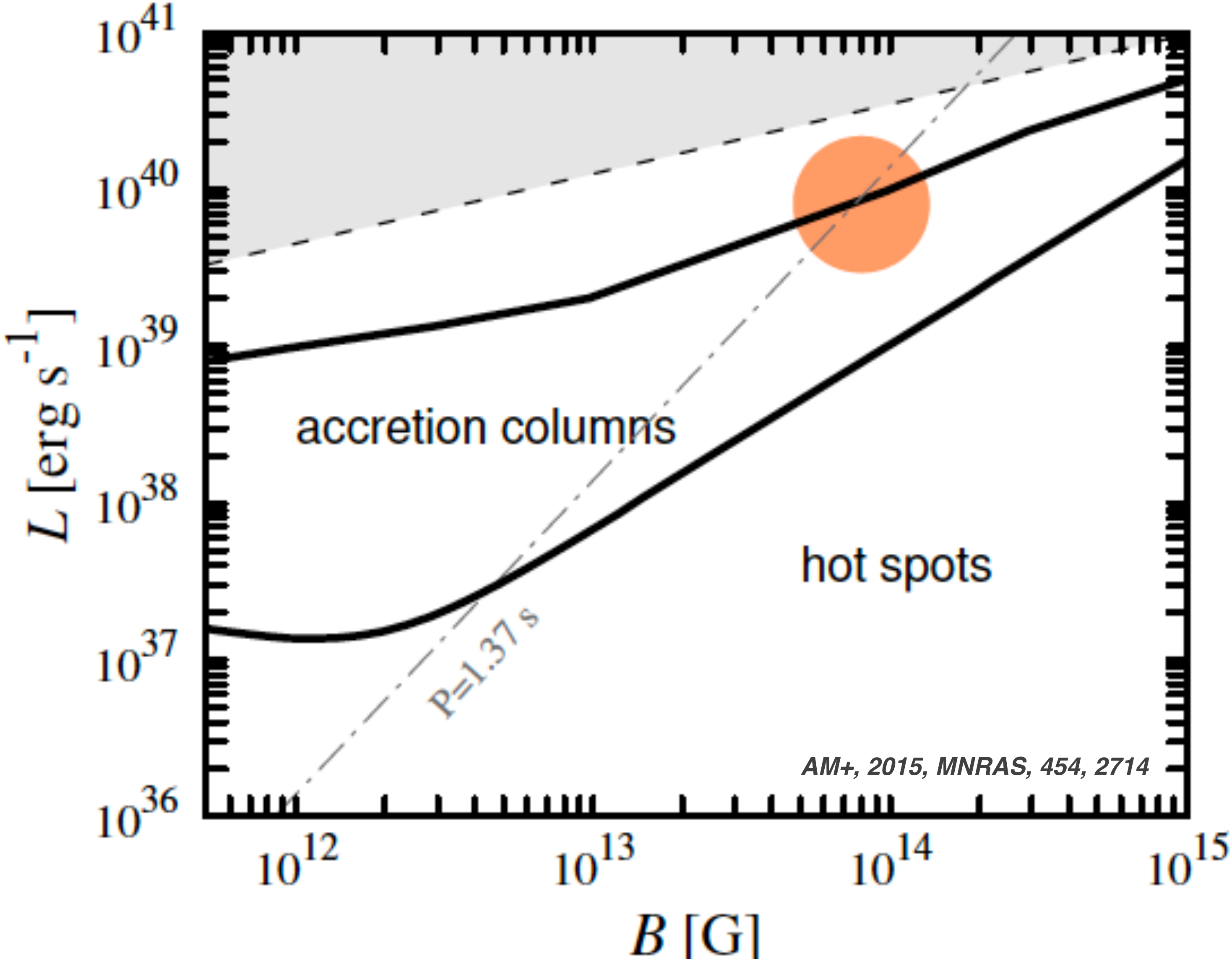

$$L_{\rm lim}(R) \simeq \frac{GM\dot{M}_{\rm lim}}{R} \simeq 4\times10^{37} k^{7/2} B_{12}^{2} P^{-7/3} M_{1.4}^{-2/3} R_{6}^{5}\ {\rm erg\ s^{-1}}$$

M82 as seen by Chandra

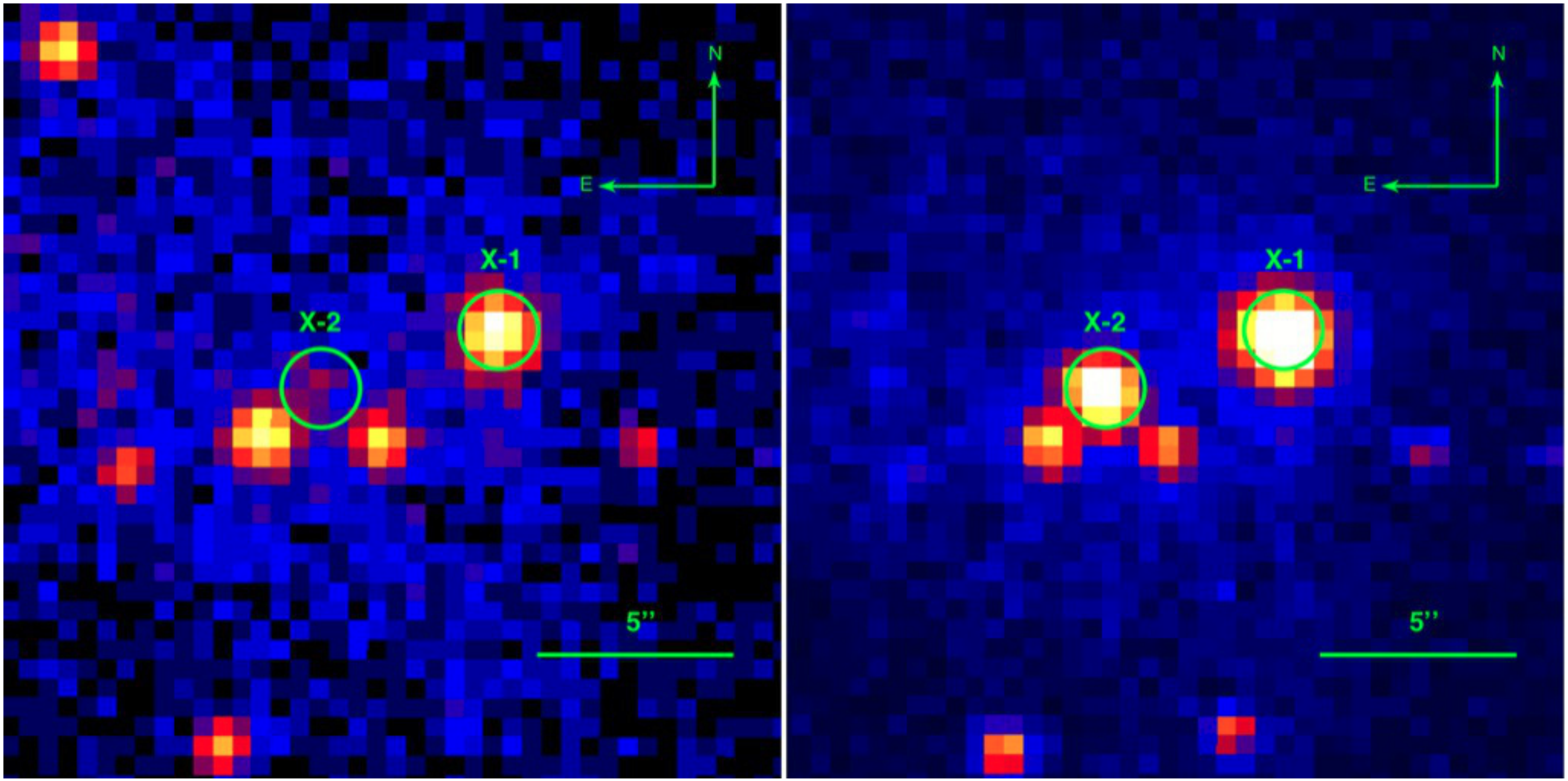

Tsygankov, AM+, 2016, MNRAS, 457

M82 X-2 intensity distribution

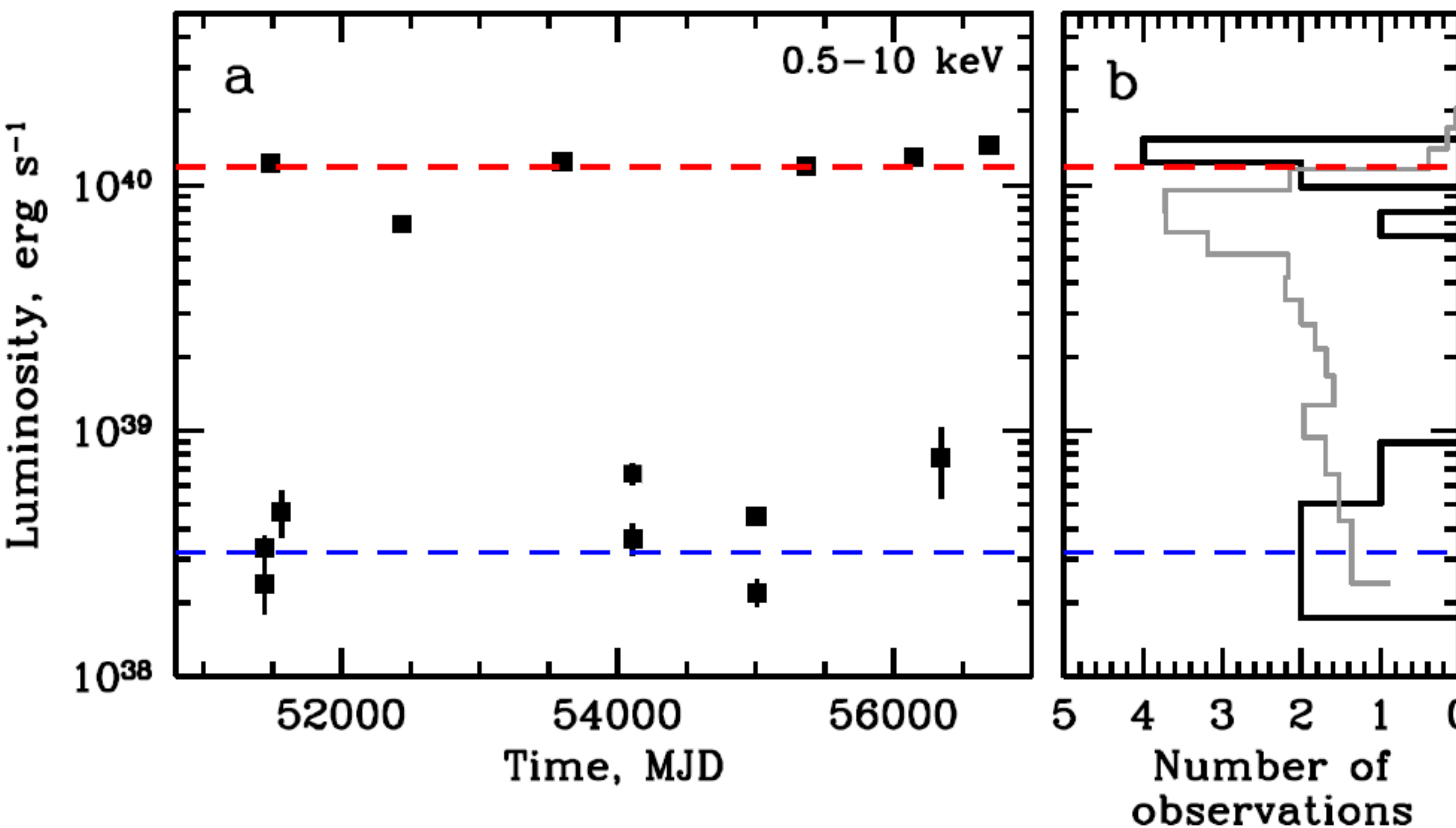

Tsygankov, AM+, 2016, MNRAS, 457

Propeller in action

$$L_{\rm lim}(R) \simeq \frac{GM\dot{M}_{\rm lim}}{R} \simeq 4\times10^{37} k^{7/2} B_{12}^{2} P^{-7/3} M_{1.4}^{-2/3} R_6^5 \,{\rm erg\,s^{-1}}$$

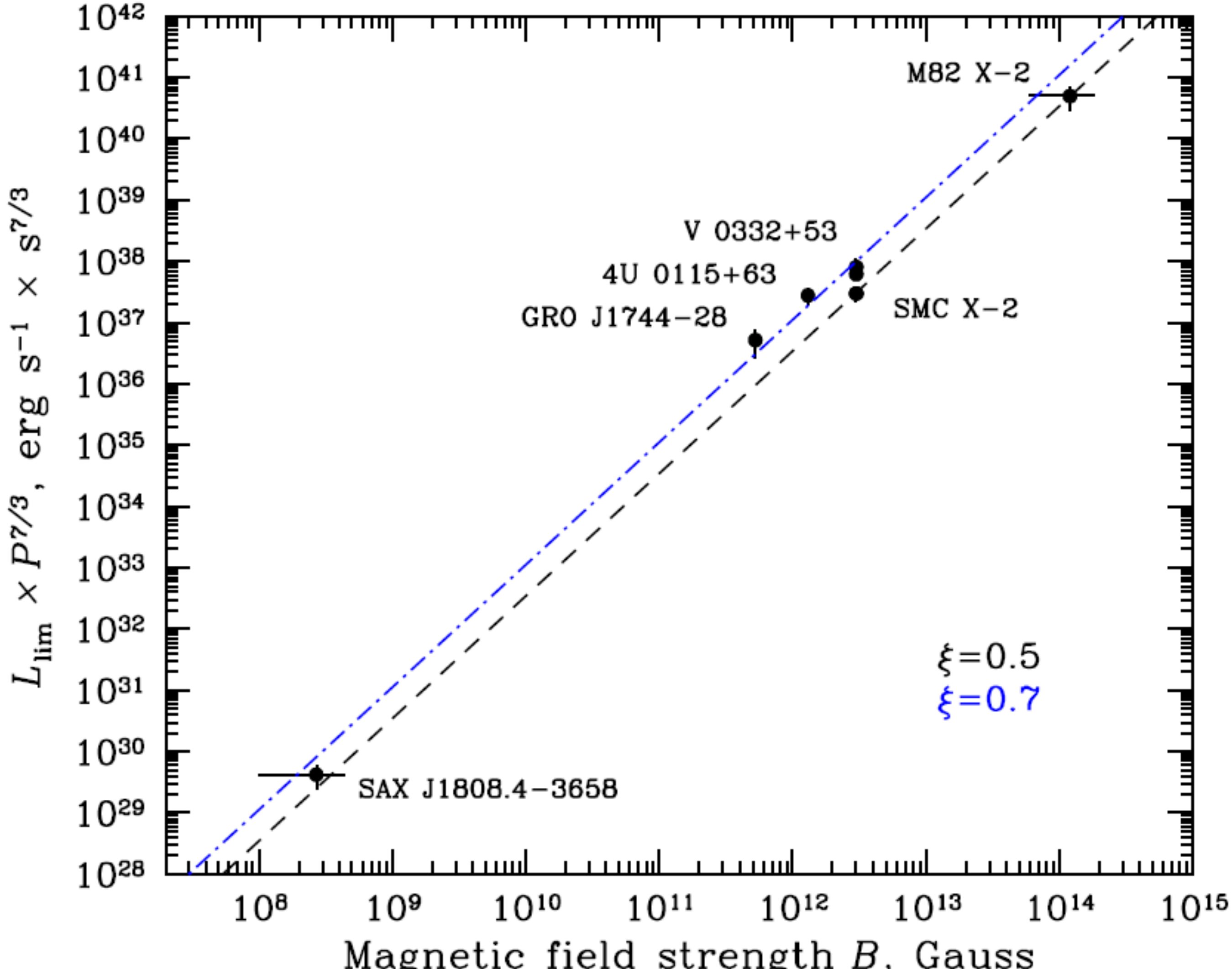

Tsygankov, AM+, 2016, MNRAS, 457

Accretion column: Advection and Neutrino pulsars

Typical time of photon escape:

$$t_{\rm diff} = \frac{\tau d}{2c} \approx 5 \times 10^{-4}\, \frac{\dot{m}_{10} d_4^2 \kappa_{\rm e}}{\beta}\ \ {\rm s}$$

$$\frac{\partial}{\partial h}\left[\left(-\frac{\rho GM}{R+h} + \frac{\rho v^2}{2} + \varepsilon_{\rm tot} + P_{\rm tot} + 2n_+ m_{\rm e} c^2\right) v\right] = Q^-$$

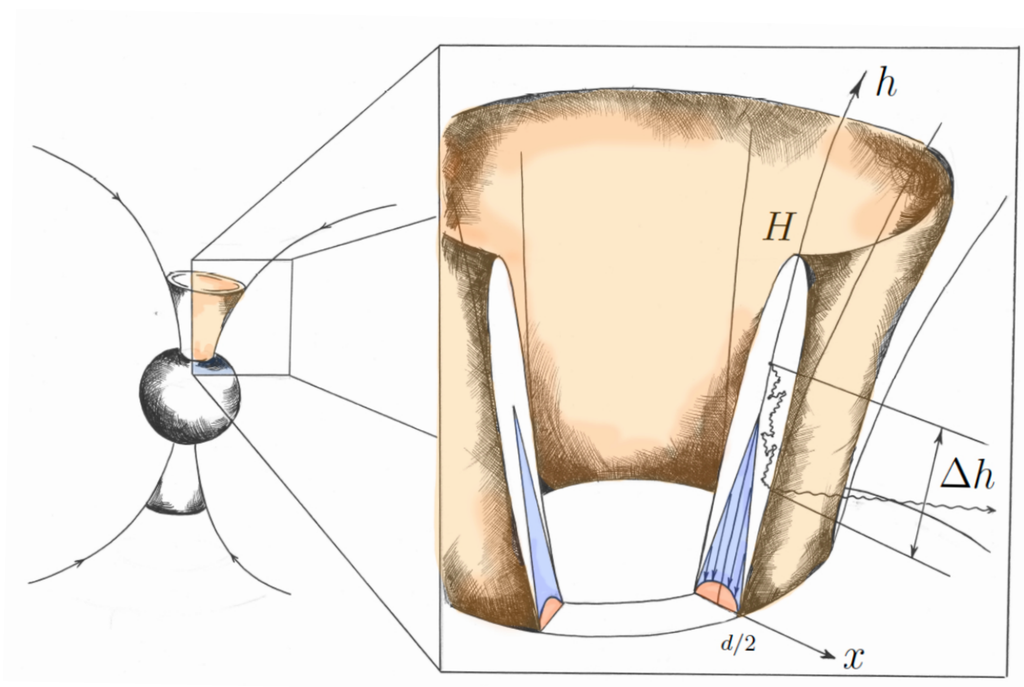

AM+, 2018, MNRAS, 476

Accretion column:
Advection and Neutrino pulsars

Typical time of photon escape:

$$t_{\rm diff} = \frac{\tau d}{2c} \approx 5\times 10^{-4}\,\frac{\dot{m}_{10} d_4^2 \kappa_{\rm e}}{\beta}\ \ {\rm s}$$

$$\frac{\partial}{\partial h}\left[\left(-\frac{\rho G M}{R+h}+\frac{\rho v^2}{2}+\varepsilon_{\rm tot}+P_{\rm tot}+2n_+ m_{\rm e} c^2\right) v\right] = Q^-$$

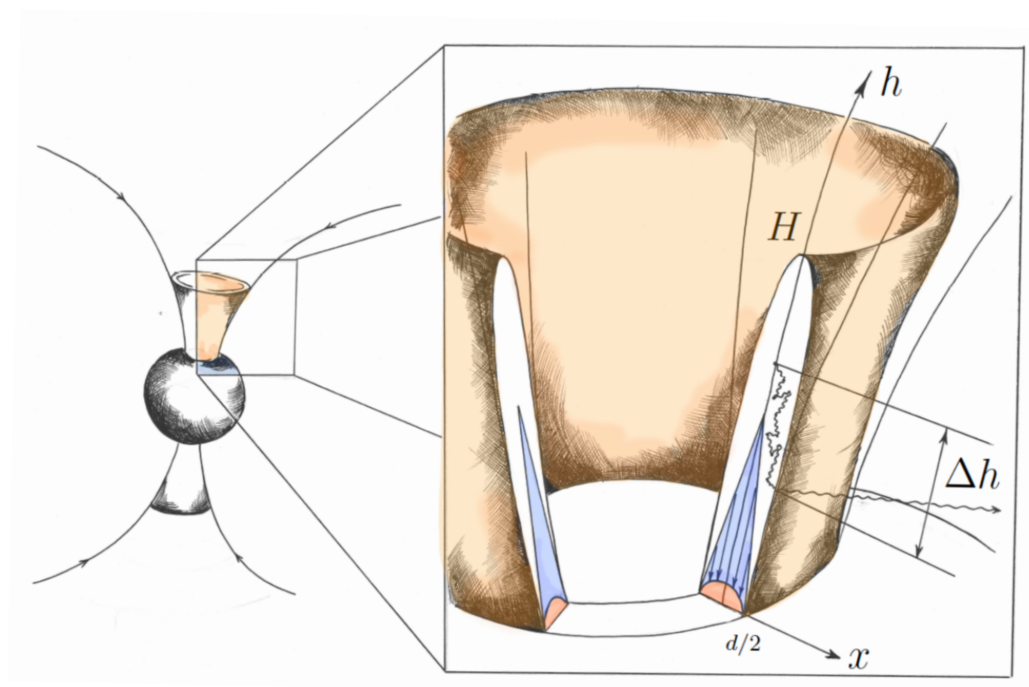

AM+, 2018, MNRAS, 476

Accretion column:
Advection and Neutrino pulsars

Typical time of photon escape:

$$t_{\rm diff} = \frac{\tau d}{2c} \approx 5 \times 10^{-4}\, \frac{\dot{m}_{10} d_4^2 \kappa_{\rm e}}{\beta}\ \ {\rm s}$$

$$\frac{\partial}{\partial h}\left[\left(-\frac{\rho G M}{R+h} + \frac{\rho v^2}{2} + \varepsilon_{\rm tot} + P_{\rm tot} + 2n_+ m_{\rm e} c^2\right) v\right] = Q^-$$

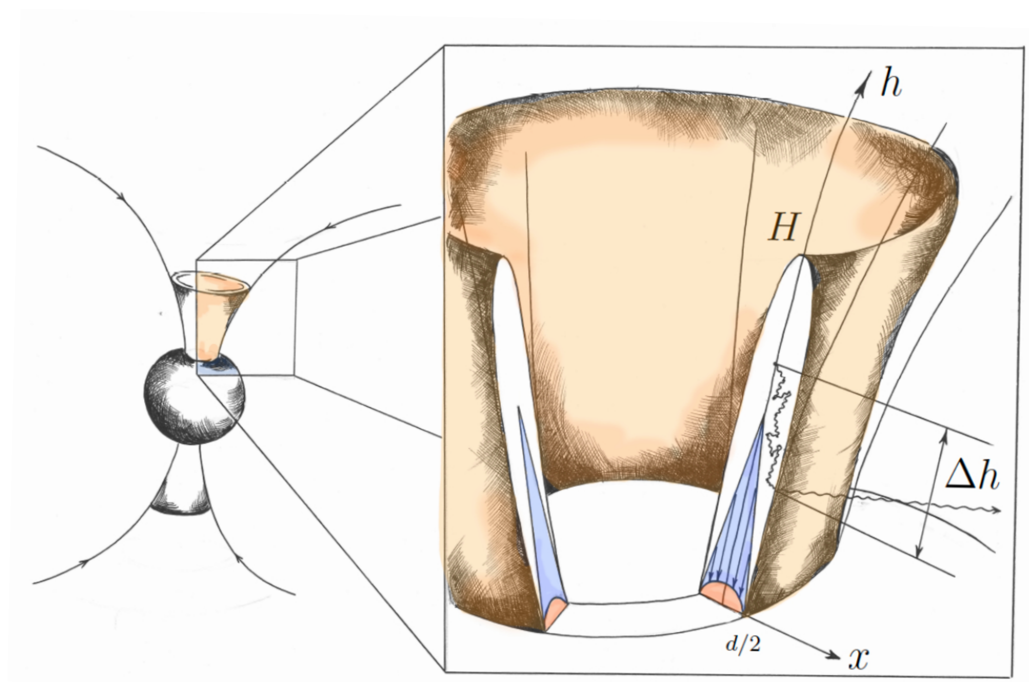

AM+, 2018, MNRAS, 476

Accretion column: Advection and Neutrino pulsars

Typical time of photon escape:

$$t_{\rm diff} = \frac{\tau d}{2c} \approx 5\times 10^{-4}\,\frac{\dot m_{10} d_4^2 \kappa_{\rm e}}{\beta}\ \ {\rm s}$$

$$\frac{\partial}{\partial h}\left[\left(-\frac{\rho G M}{R+h} + \frac{\rho v^2}{2} + \varepsilon_{\rm tot} + P_{\rm tot} + 2n_+ m_{\rm e} c^2\right) v\right] = Q^-$$

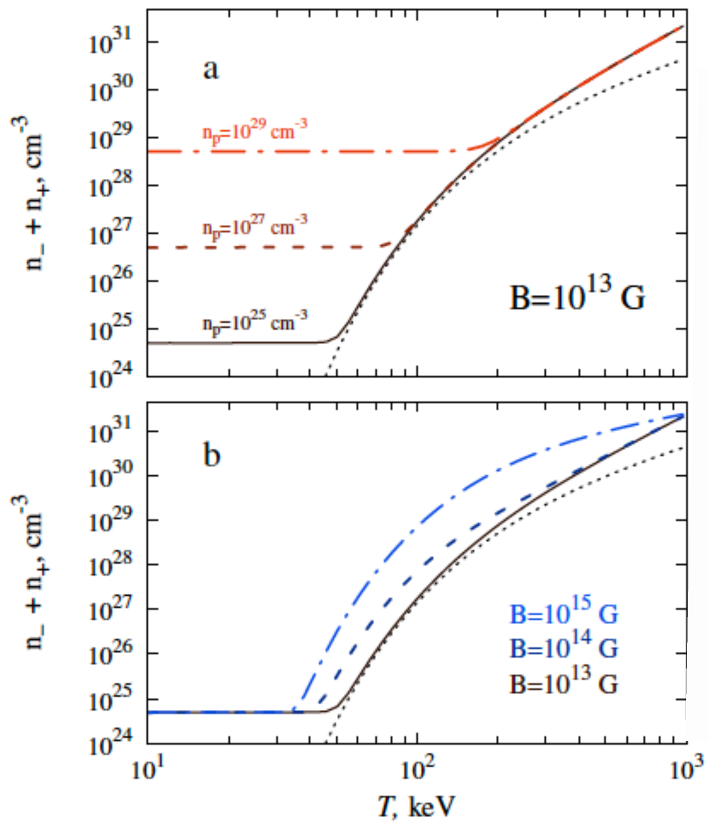

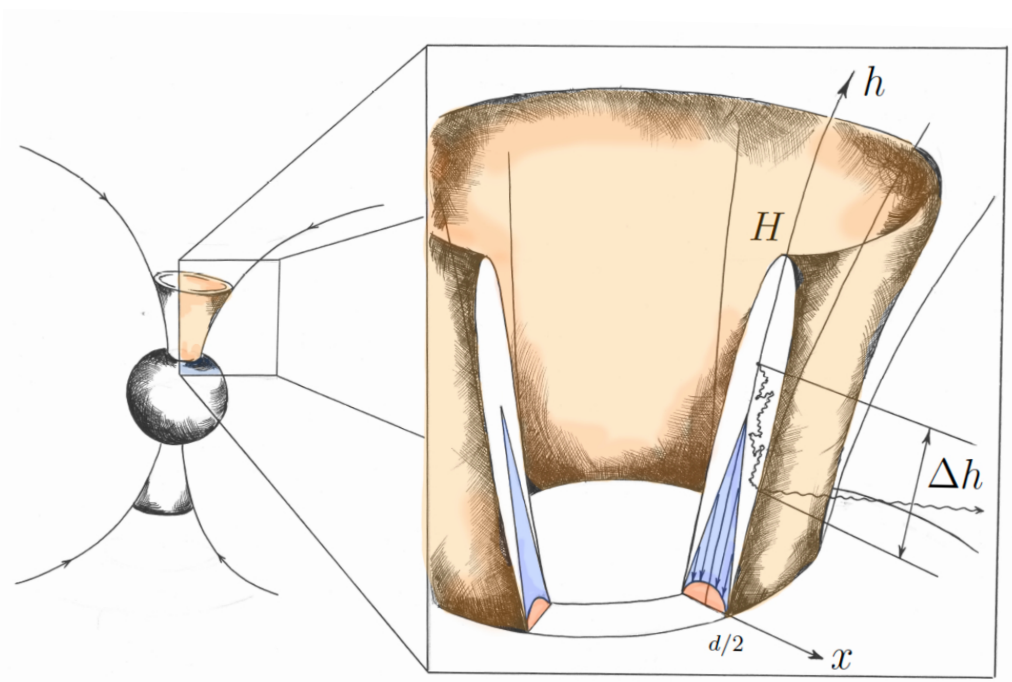

AM+, 2018, MNRAS, 476

Accretion column:
Advection and Neutrino pulsars

Typical time of photon escape:

$$t_{\rm diff} = \frac{\tau d}{2c} \approx 5\times 10^{-4}\,\frac{\dot m_{10} d_4^2 \kappa_{\rm e}}{\beta}\ \ {\rm s}$$

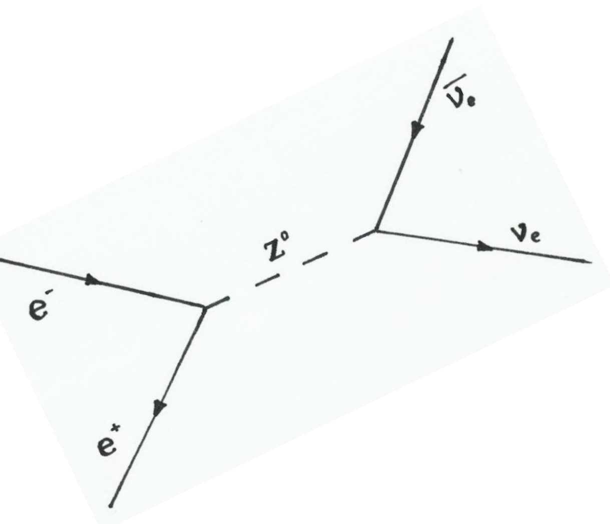

$$\frac{\partial}{\partial h}\left[\left(-\frac{\rho G M}{R+h}+\frac{\rho v^2}{2}+\varepsilon_{\rm tot}+P_{\rm tot}+2n_+ m_{\rm e}c^2\right)v\right]=Q^-$$

$$e^- + e^+ \longrightarrow \nu + \overline{\nu}$$

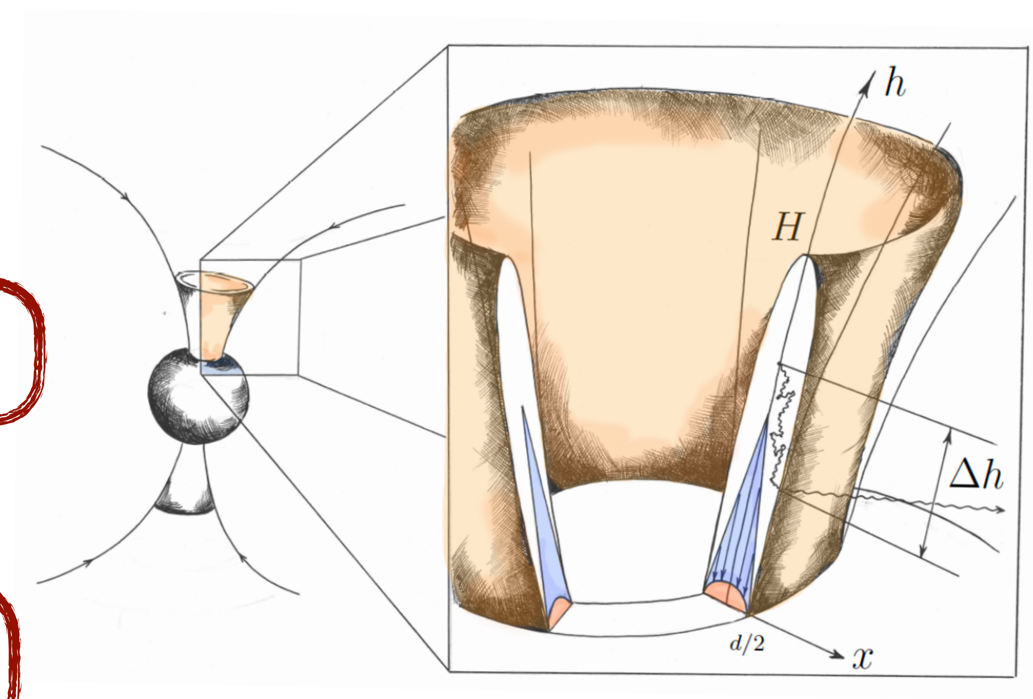

The total accretion luminosity:

$$L_{\rm tot} = \frac{GM\dot M}{R} = L_{\rm ph} + L_\nu$$

AM+, 2018, MNRAS, 476

Accretion column: Photon and Neutrino Luminosity

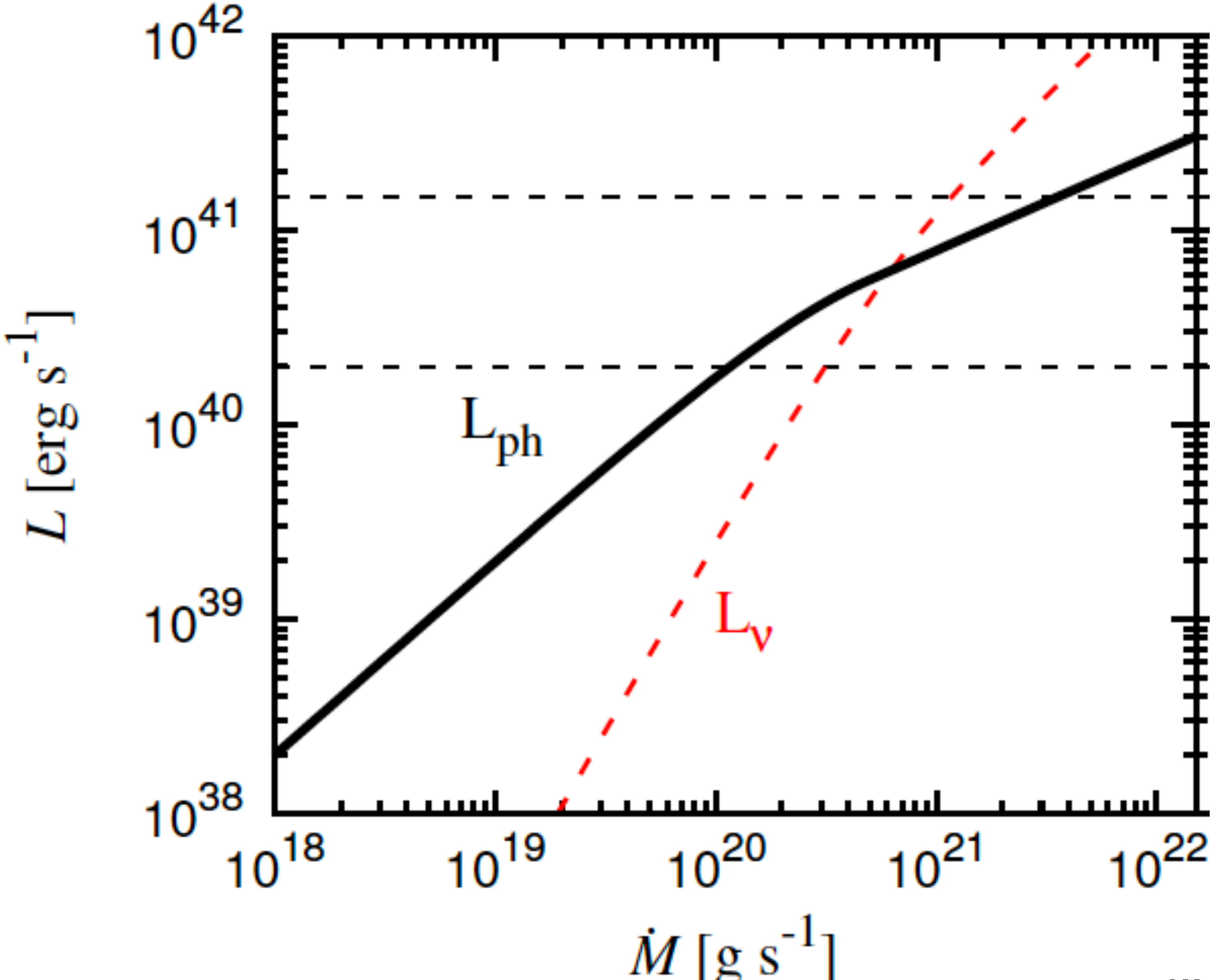

AM+, 2018, MNRAS, 476

Outflows from accretion discs in ULX pulsars

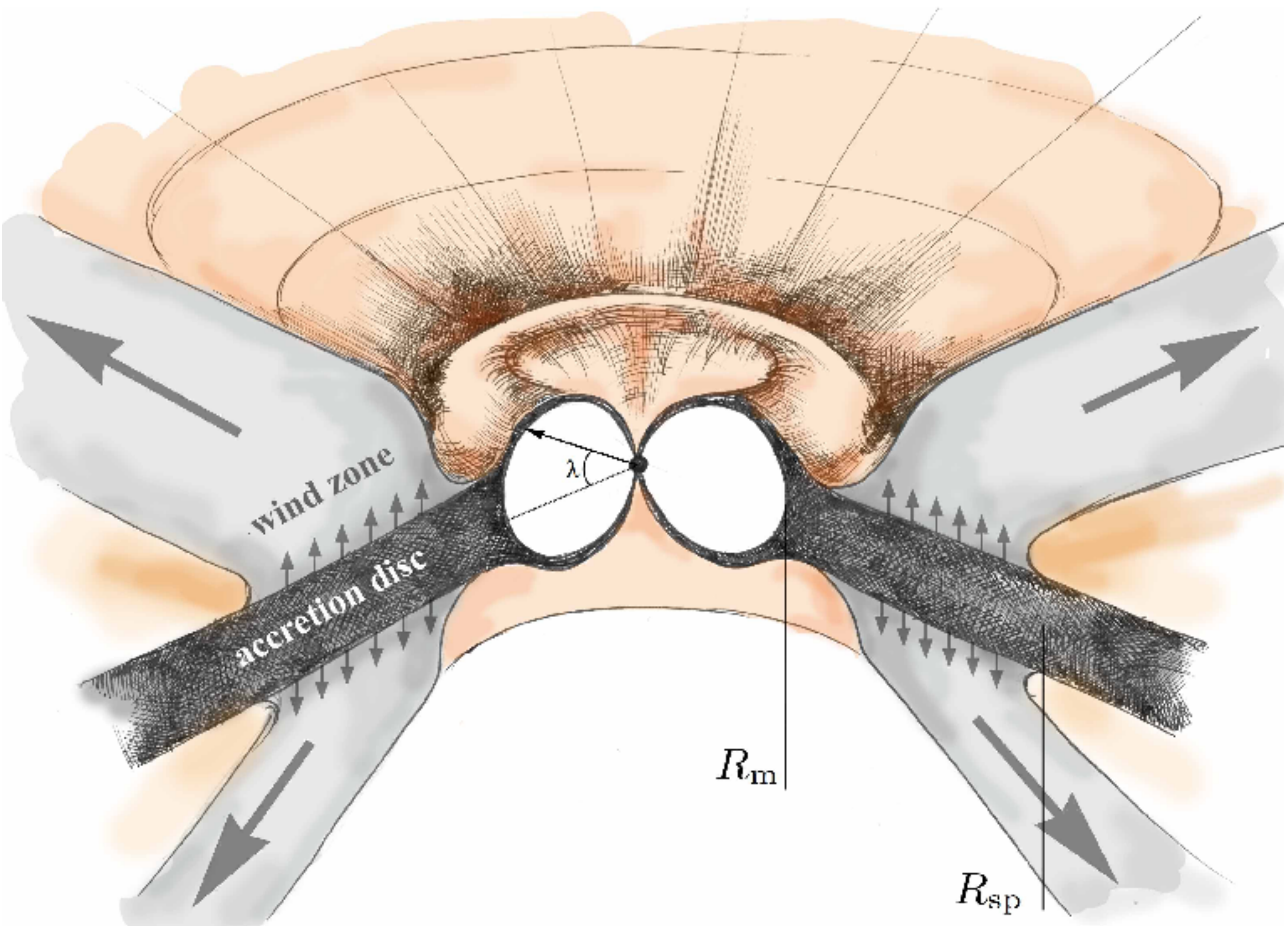

AM+, 2017, MNRAS, 467
AM+, 2019, MNRAS, 484

Geometrical Beaming vs. Pulsed Fraction

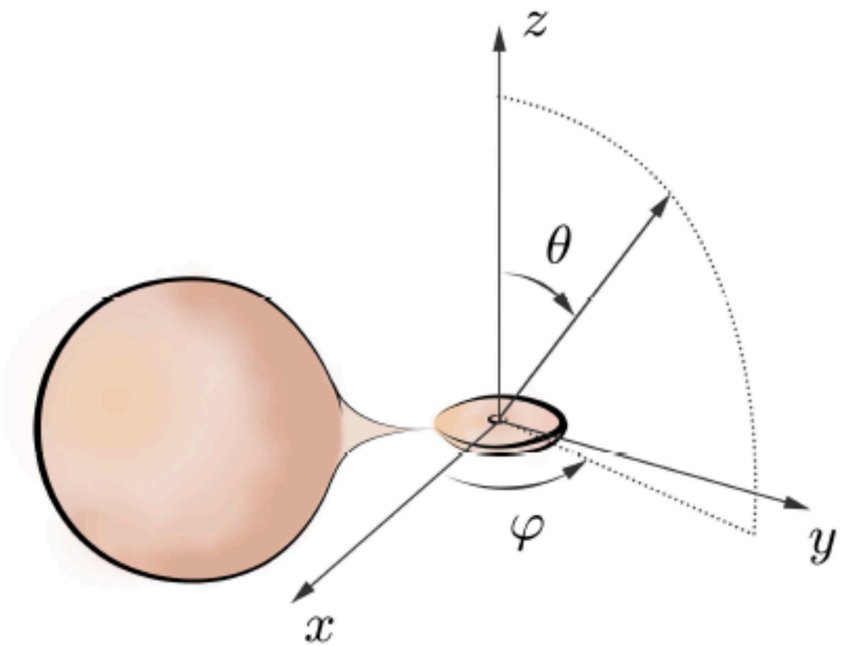

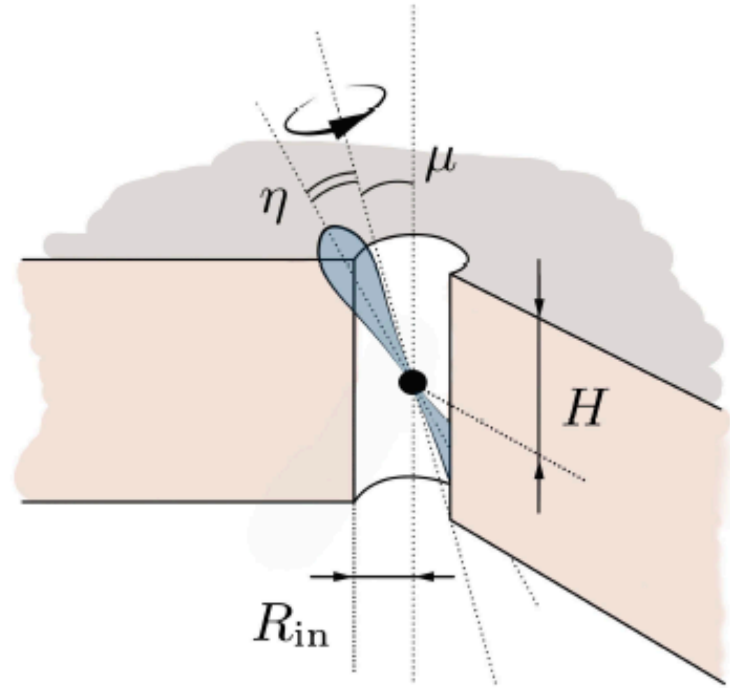

We know **5 pulsating ULXs**.
But, there are only **~15 ULXs** out of **~300** provide the statistics sufficient for detection of pulsations.
(see, e.g., Rodrigues Castillo+, 2020, ApJ, 895)

High Pulsed Fraction (~10 percents and more) is a typical feature of ULX pulsars.

AM+, 2021, MNRAS, 501

Geometrical Beaming vs. Pulsed Fraction

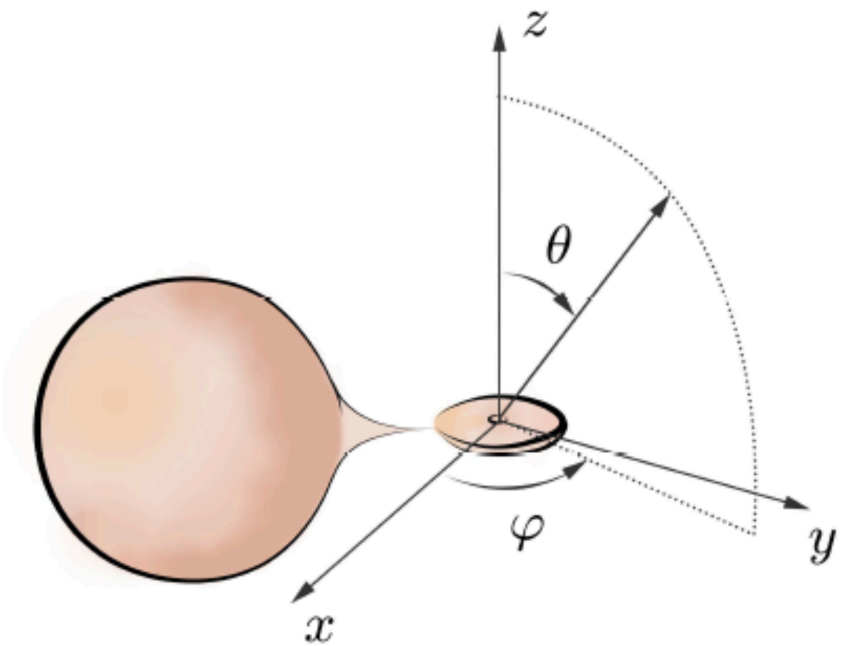

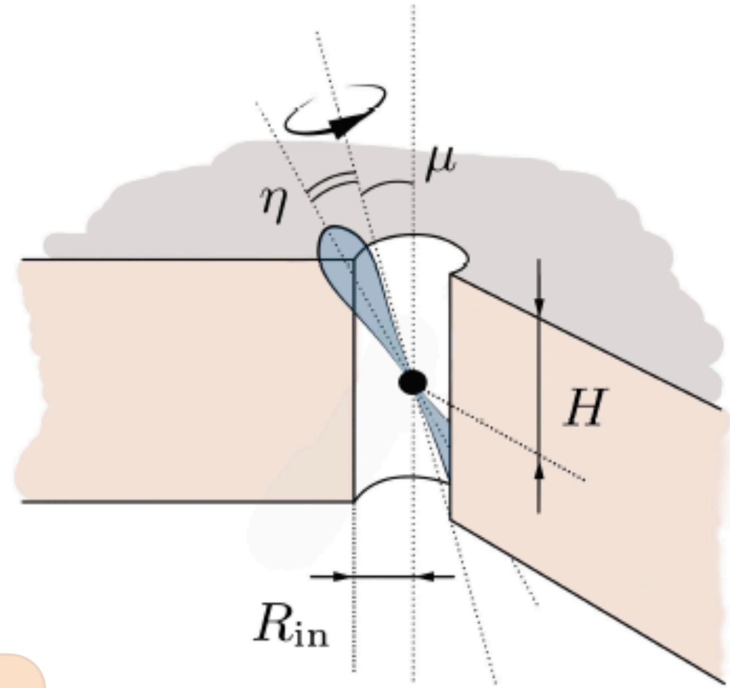

*A certain **beam geometry** from a NS*
***Parameters of rotation** in respect to the accretion flow*
***H/R** parameter*

We use Monte Carlo simulations and trace photons accounting for:
GR effects
&
reflection of photons from the walls of accretion funnel

We reproduce the pulse profiles for different observers

AM+, 2021, MNRAS, 501

Distribution of ULX pulsars over the PF and Luminosity Amplification Factor

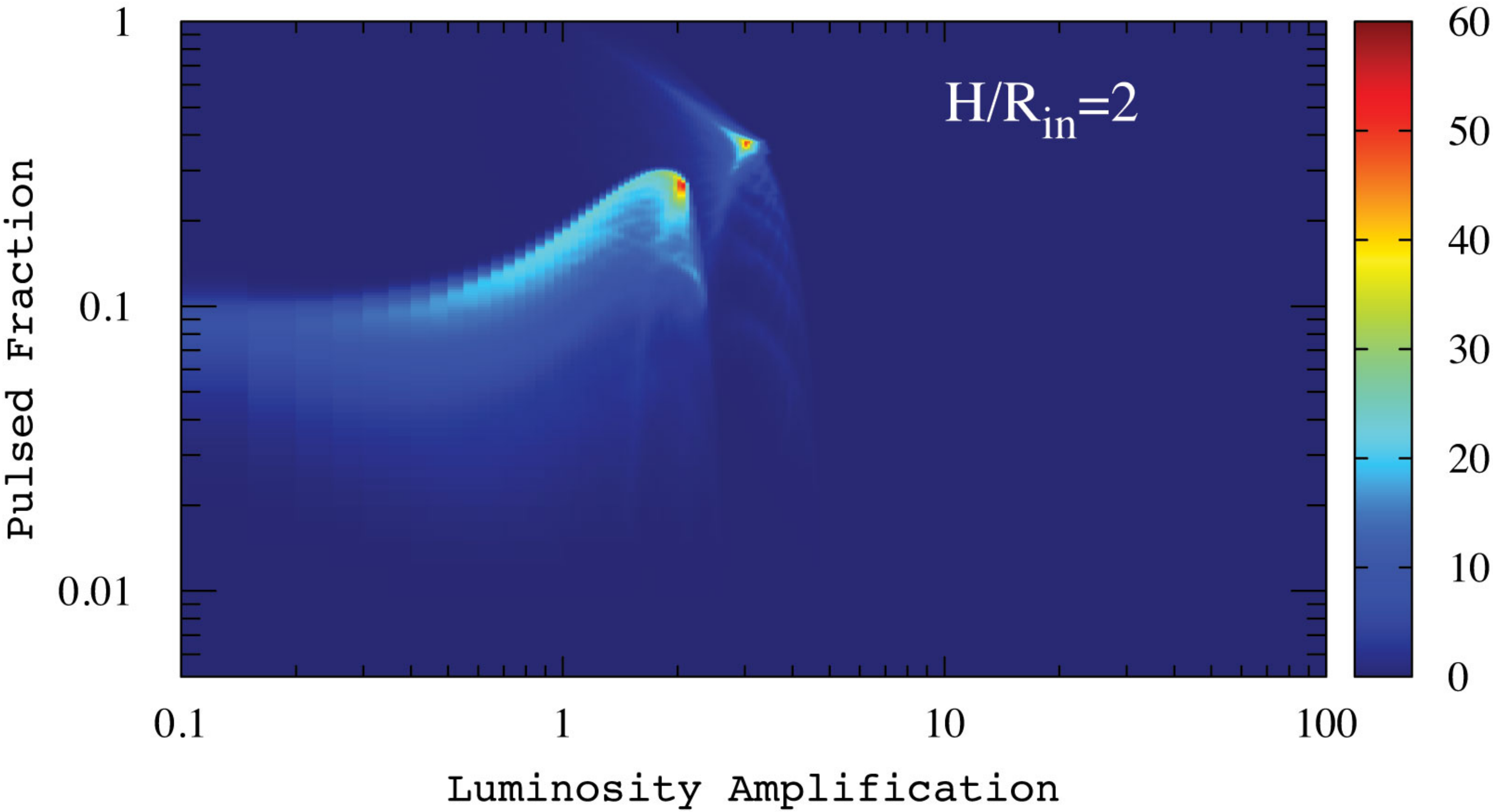

AM+, 2021, MNRAS, 501

Distribution of ULX pulsars over the PF and Luminosity Amplification Factor

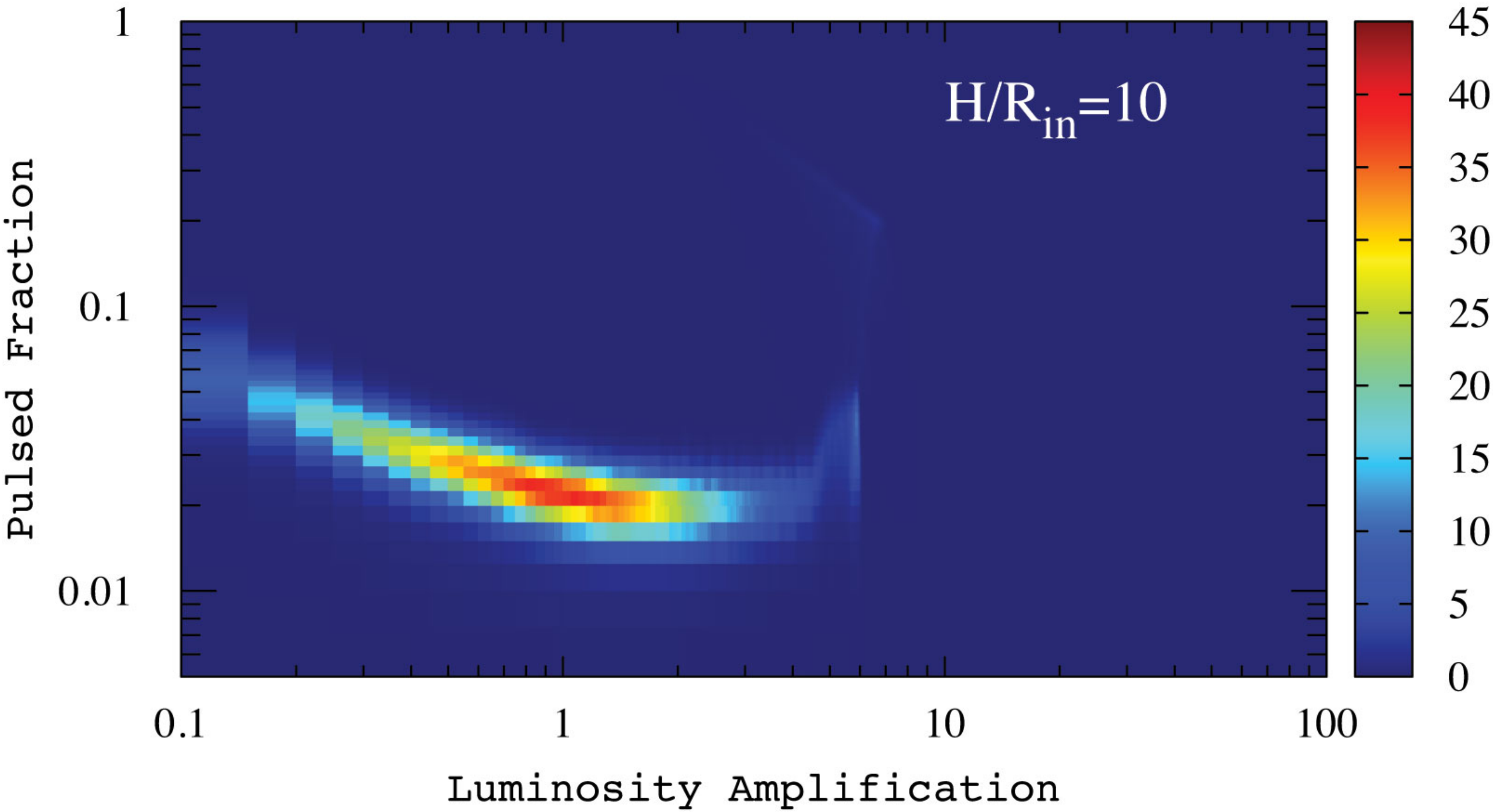

AM+, 2021, MNRAS, 501

Distribution of ULX pulsars over the PF and Luminosity Amplification Factor

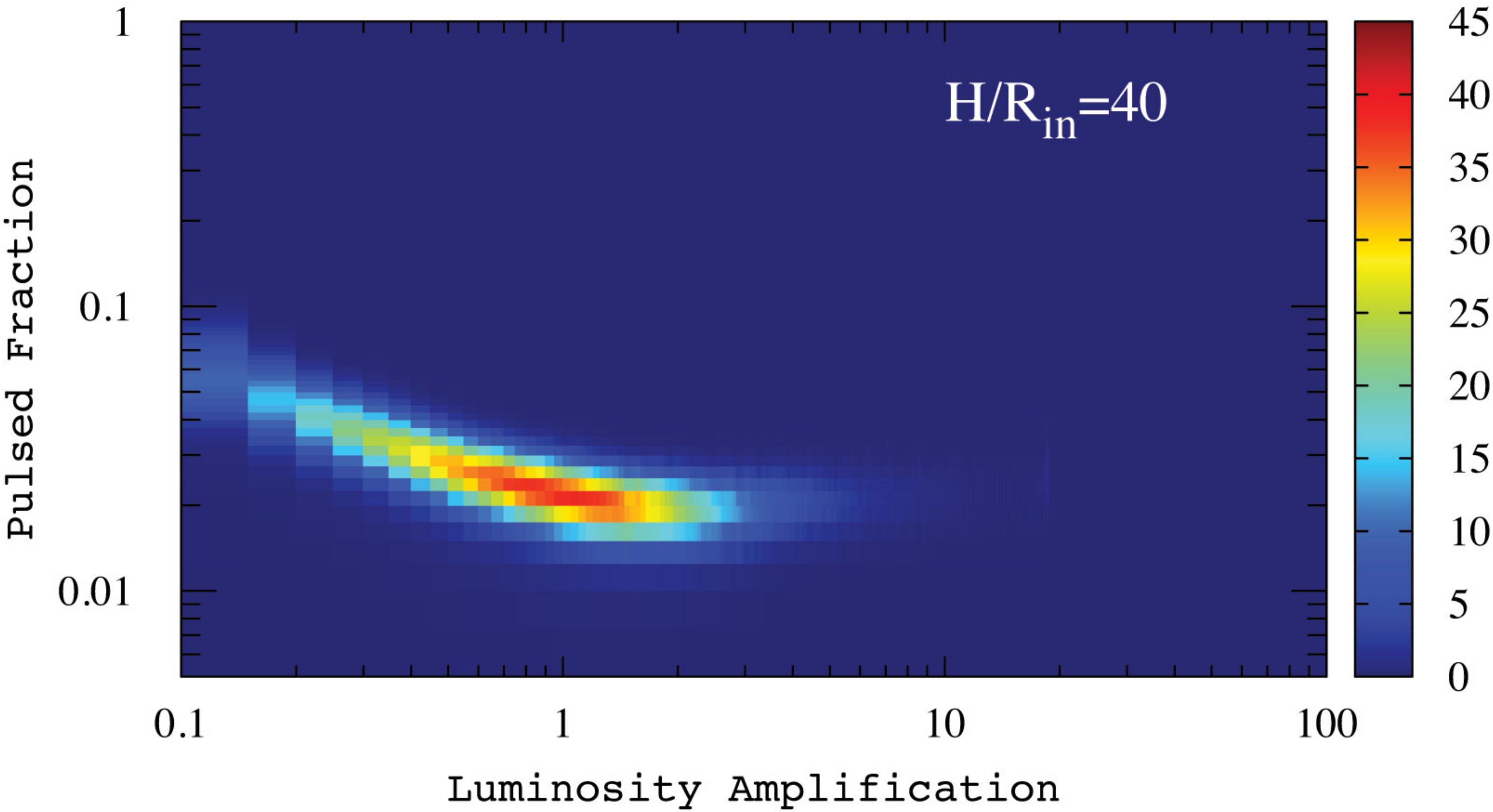

AM+, 2021, MNRAS, 501

Accretion envelope

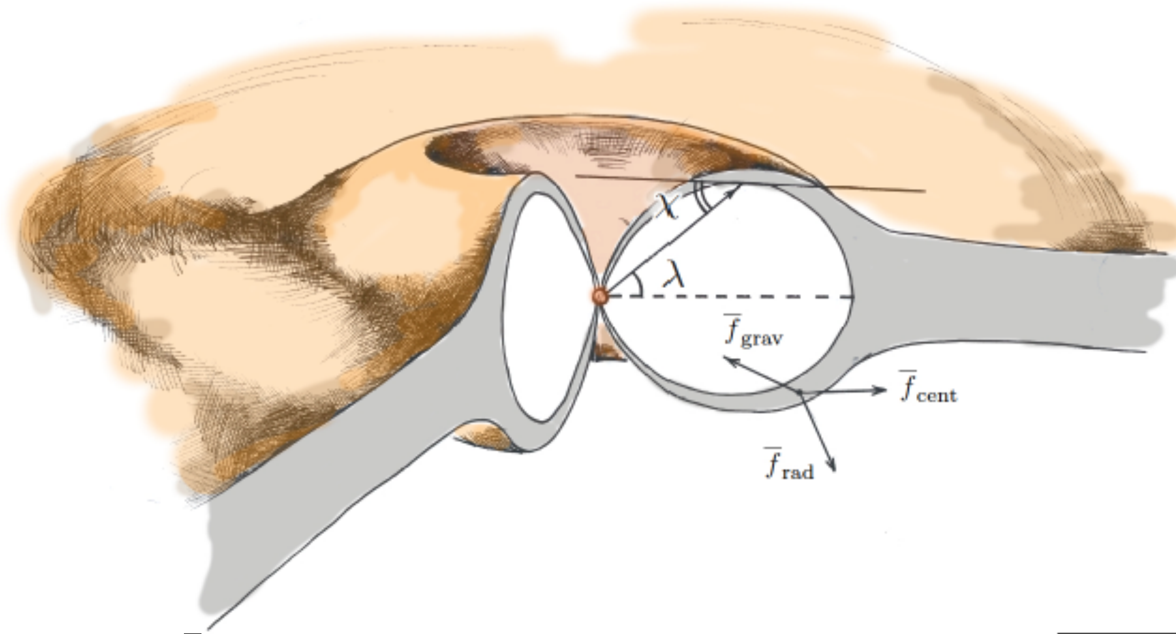

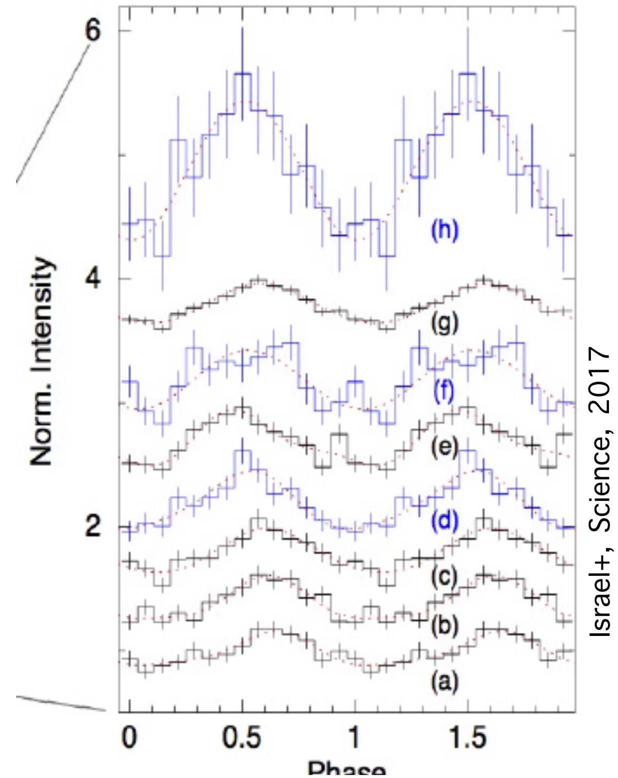

Important consequences:

(1) we do not see directly the central NS in ULX pulsars;

(2) **smooth pulse profiles** and hardly detected **cyclotron lines;**

(3) **the energy spectra** of ULXPs are affected by multiple scatterings in the envelope;

(4) suppressed **power spectra** at high Fourier frequency;

(5) **super-orbital variability** because of precession of magnetic dipole.

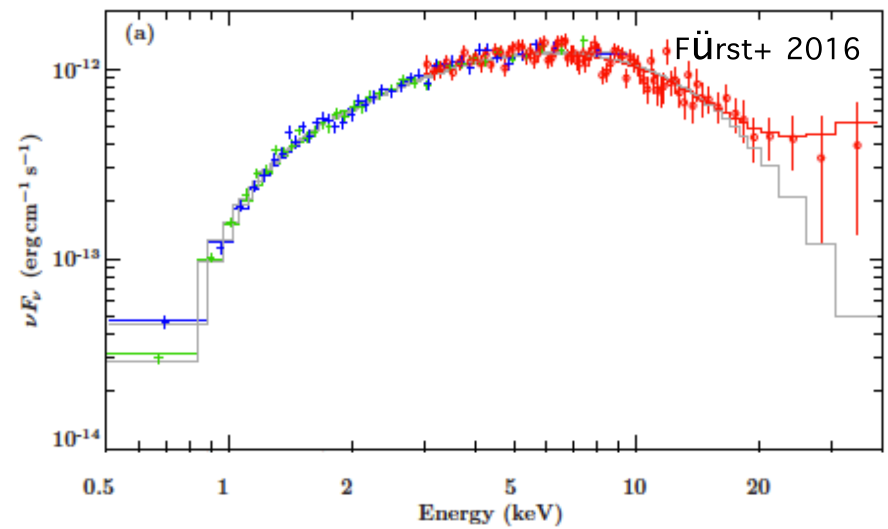

AM+, 2017, MNRAS, 467
AM+, 2019, MNRAS, 484

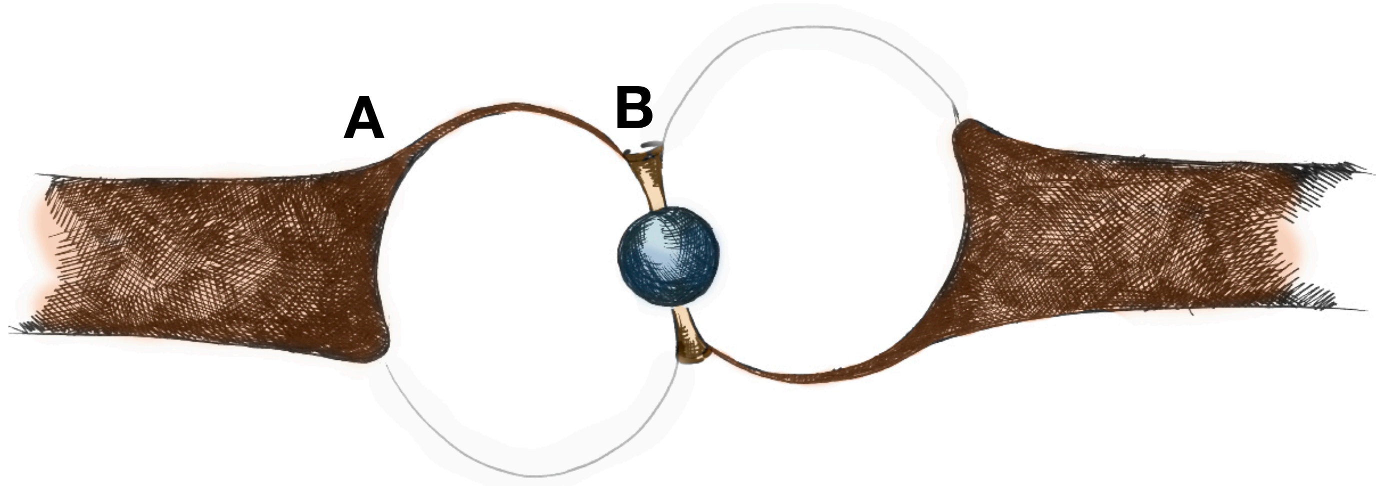
A
B

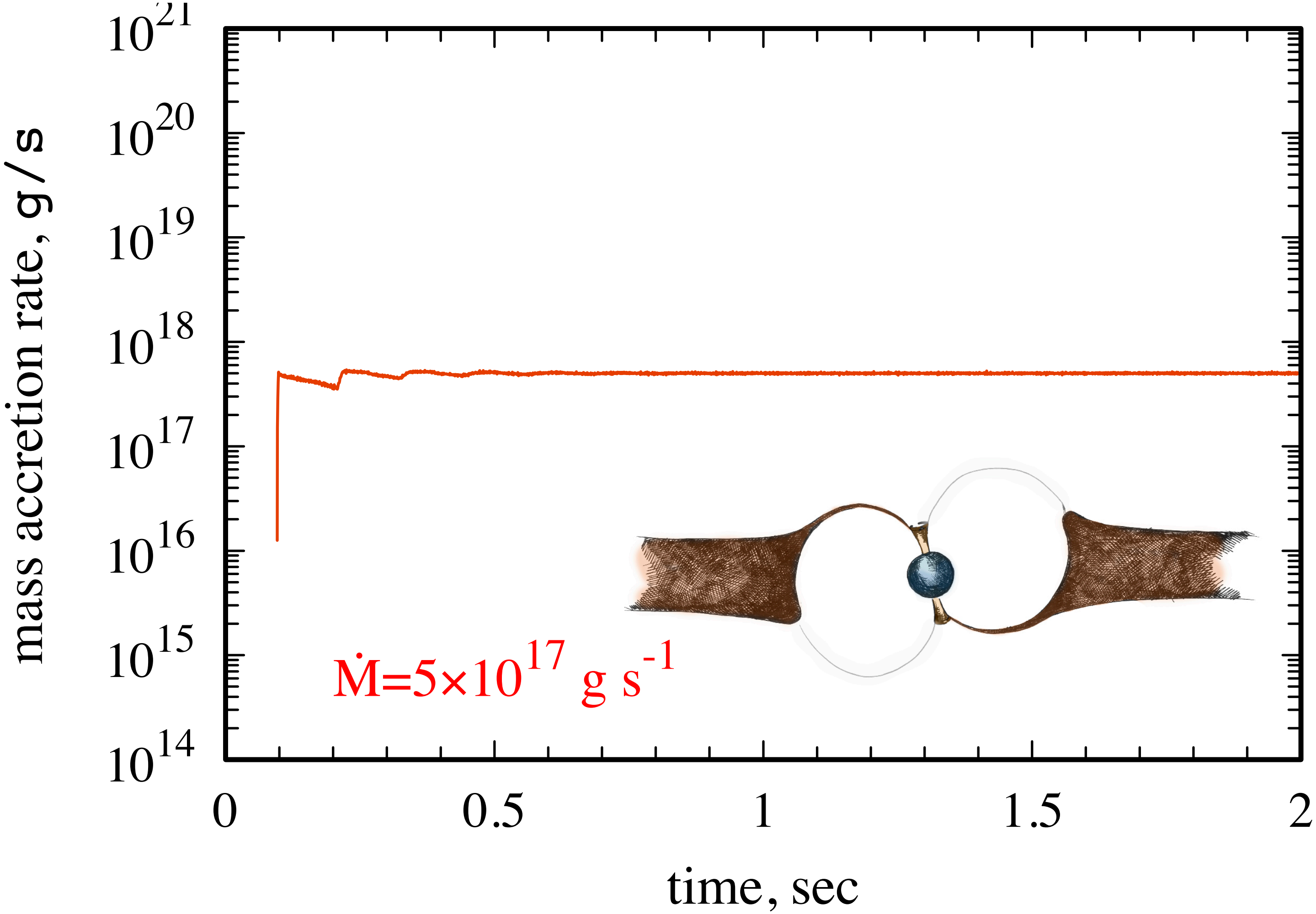

mass accretion rate, g/s
10^{21}
10^{20}
10^{19}
10^{18}
10^{17}
10^{16}
10^{15}
10^{14}
0
0.5
1
1.5
2
time, sec
$\dot{M}=5\times10^{17}$ g s^{-1}

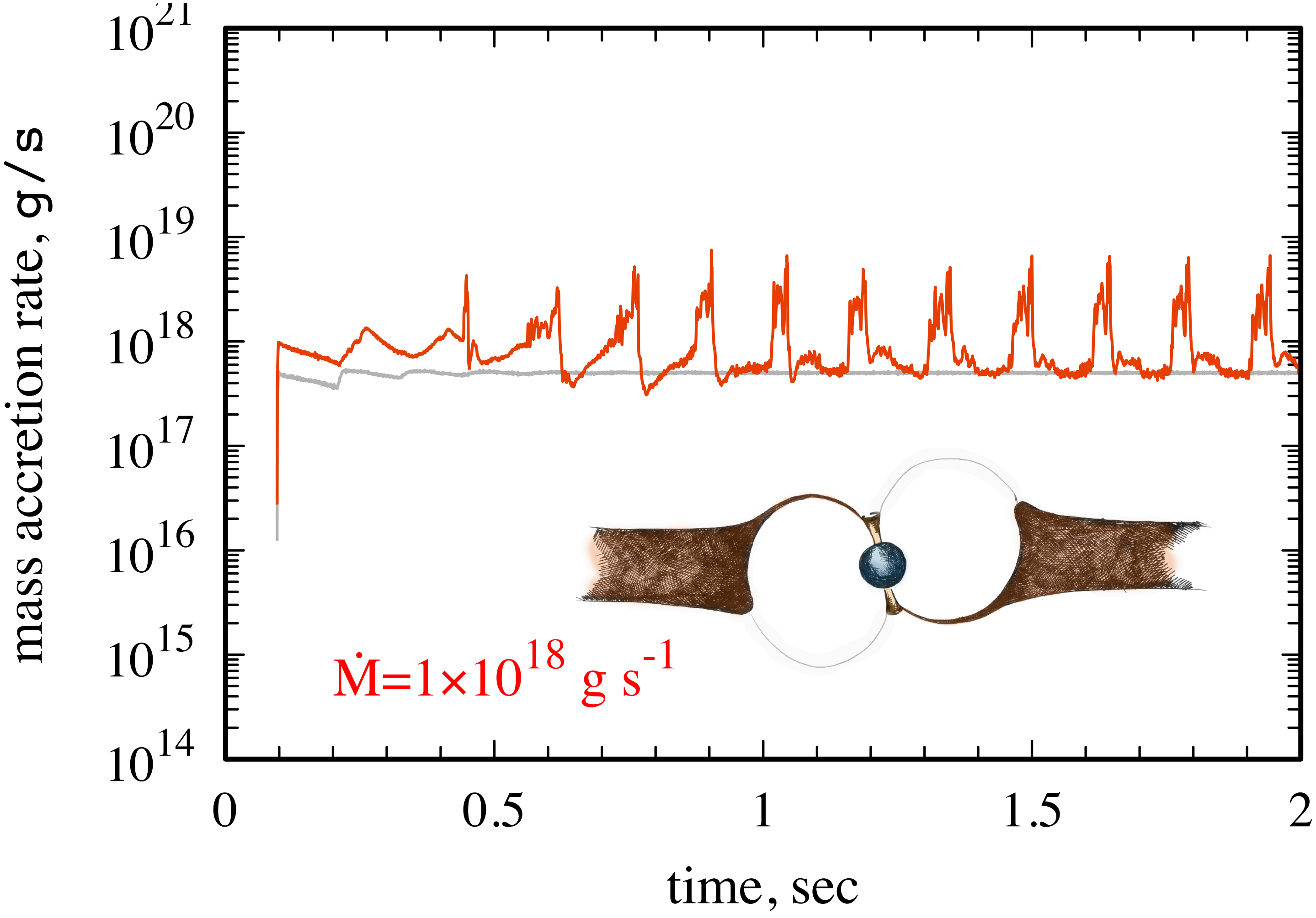

mass accretion rate, g/s
time, sec
$\dot{M}=1\times10^{18}$ g s^{-1}

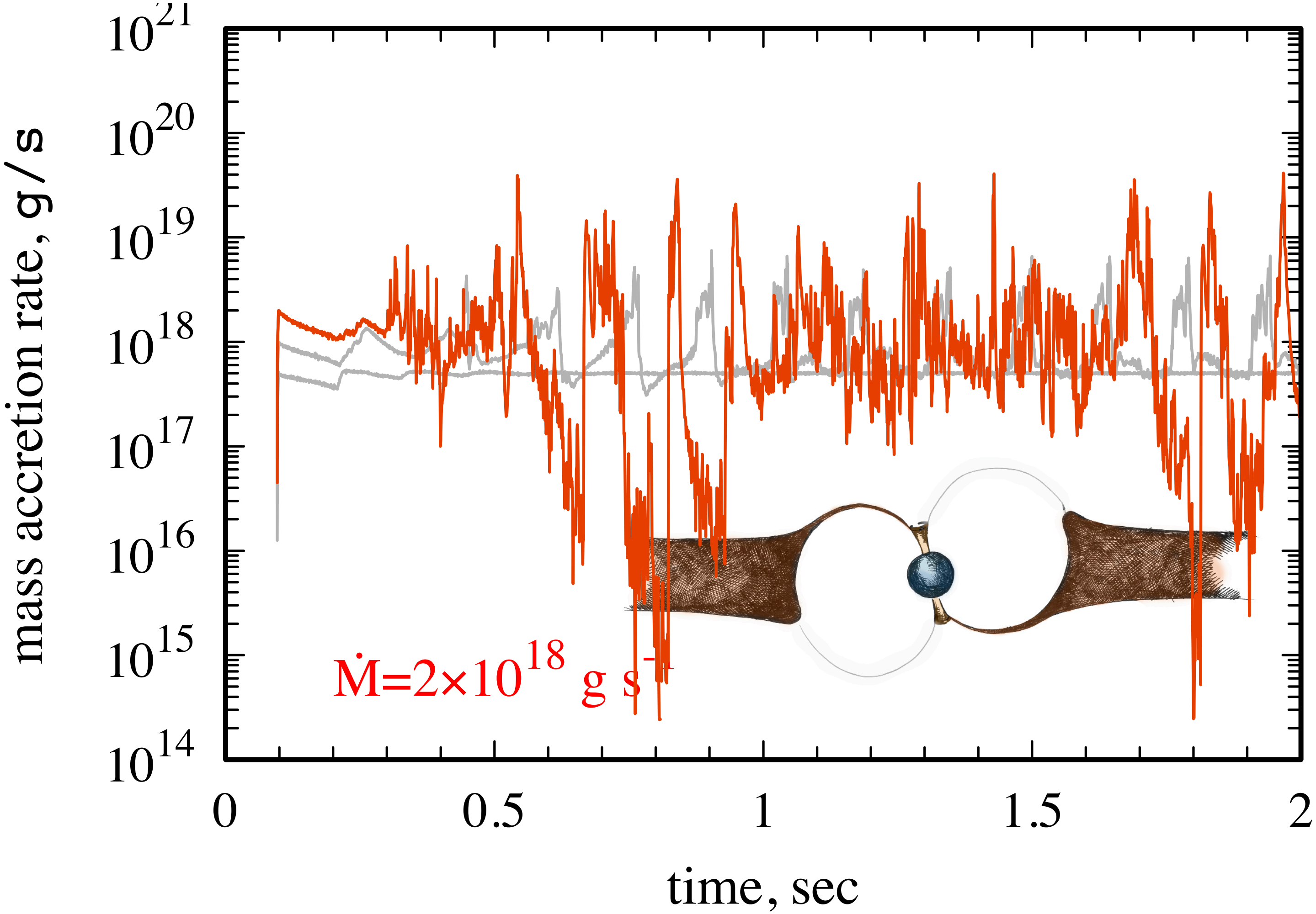

mass accretion rate, g/s
10^{21}
10^{20}
10^{19}
10^{18}
10^{17}
10^{16}
10^{15}
10^{14}
0
0.5
1
1.5
2
time, sec
$\dot{M}=2\times10^{18}$ g s^{-1}

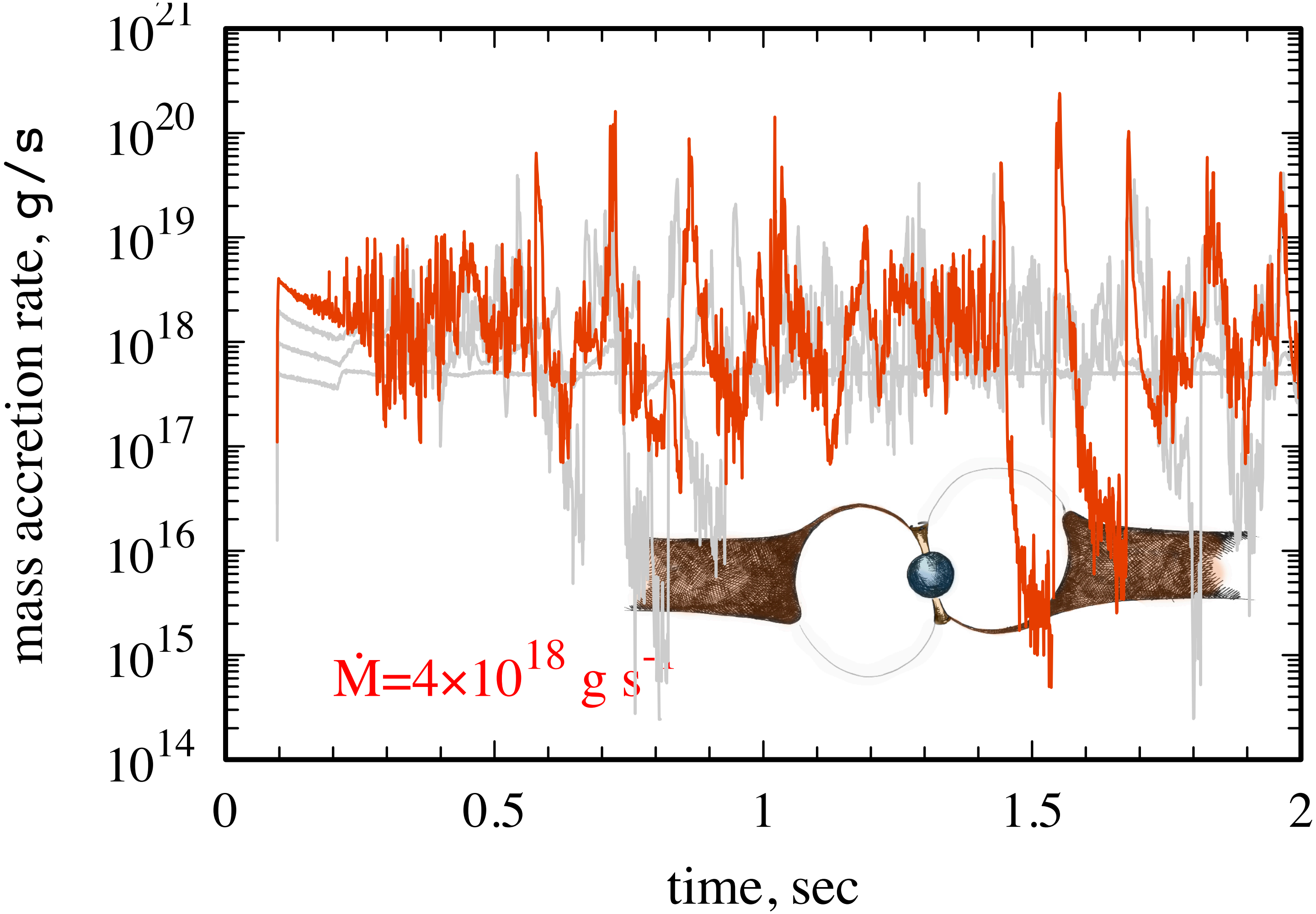

mass accretion rate, g/s
10^21
10^20
10^19
10^18
10^17
10^16
10^15
10^14
0
0.5
1
1.5
2
time, sec
Ṁ=4×10^18 g s^-1

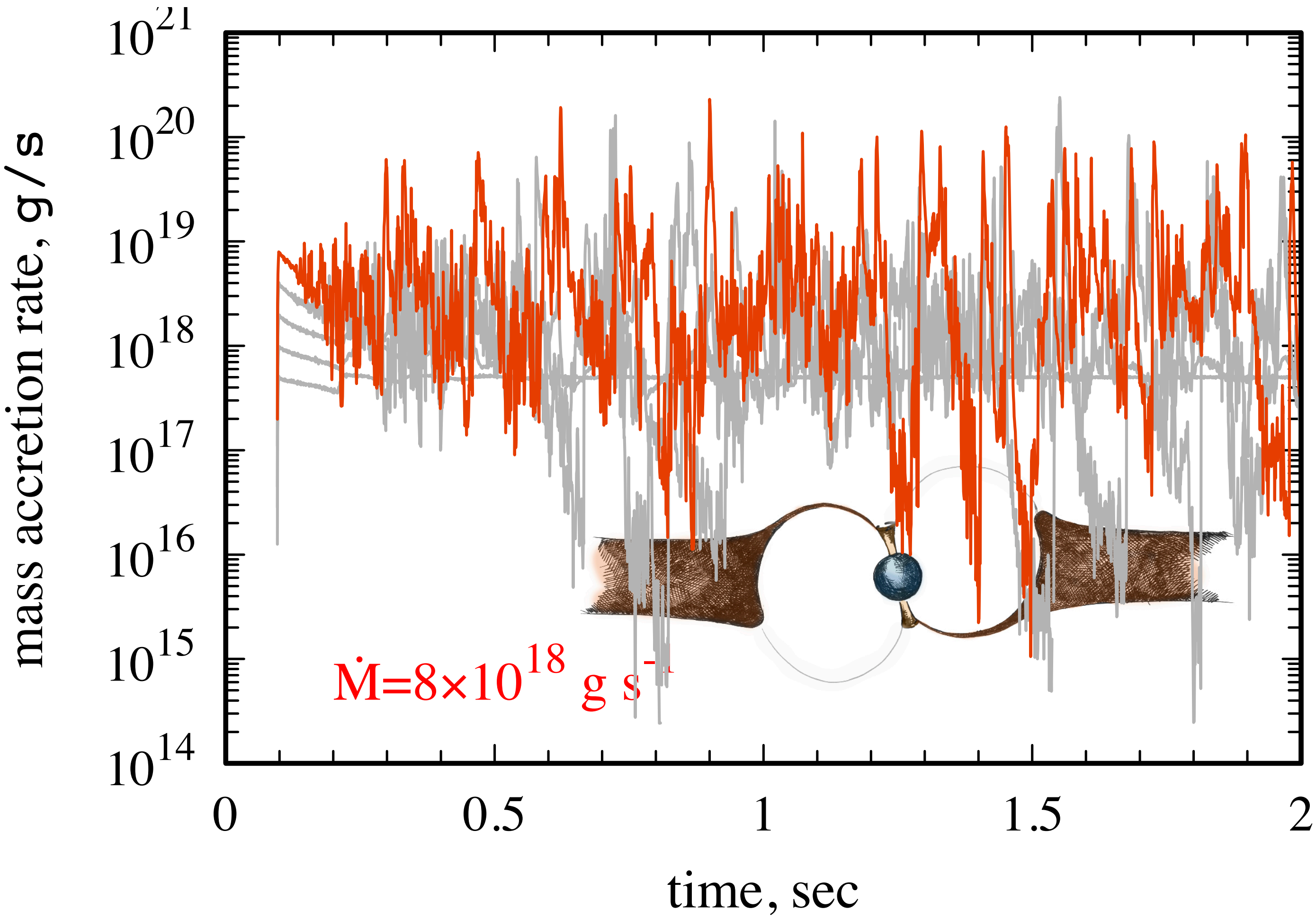
mass accretion rate, g/s
time, sec
$\dot{M}=8\times10^{18}$ g s^{-1}
10^21
10^20
10^19
10^18
10^17
10^16
10^15
10^14
0
0.5
1
1.5
2

Short Summary

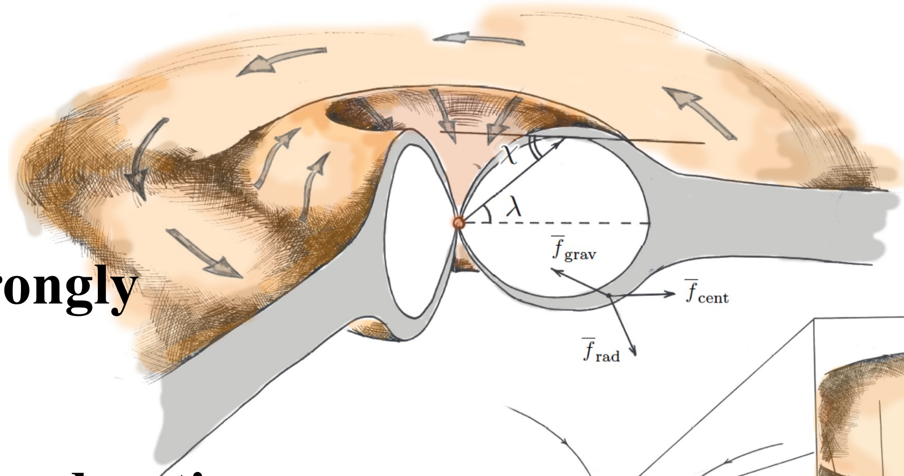

(1) Accretion columns are the central engines in ULXs; their luminosity is strongly affected by geometry of accretion channel;

(2) The column becomes advective at extreme mass accretion rates; advective columns can produce strong neutrino emission;

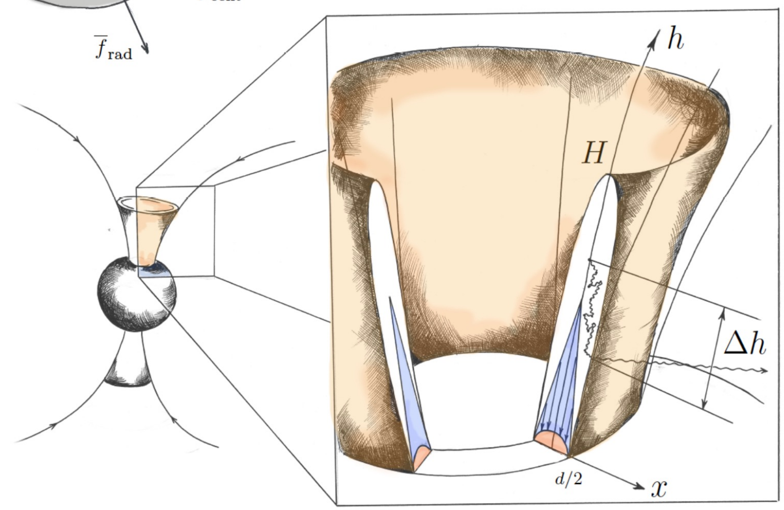

(3) Bright ULX pulsars are surrounded by optically thick envelopes. The envelopes determine the observational manifestation of ULX pulsars;

(4) Strong outflow from the accretion disc in ULX pulsars is possible in the case of relatively weak dipole component of magnetic field

But

many and many details remain unclear and/or debated.

(1) magnetic field strength

(2) evolutionary status of ULX pulsars

(3) fraction of NS among ULXs

(4) fate of a companion star

(5) …